Polarization in Noble Gases 2026
Magnetometry Tutorial

Mark Limes
Associate Prof.
Virginia Tech
4/22/2026

Magnetometry Tutorial

- General Magnetometry
- Optical Pumping of Metastable Noble gas electronic states (2^3S_1 in ^4He),

  direct optical read-out
- Metastability Exchange Optical Pumping (MEOP) of Noble gas Nuclei,
- Spin Exchange Optical Pumping (SEOP) of Noble gas Nuclei,

  both external read-out via:

  a) coils

  b) SQUIDs or

  c) atoms (can use atoms for in-situ measurements, optically detected)

Magnetometry

- Magnetic field torques spins $\vec{\tau} = \vec{M} \times \vec{B}$

$$P_{+1/2} \propto \frac{1}{(\gamma B)^2 + \Gamma^2}$$

$$\omega = \gamma B_x$$

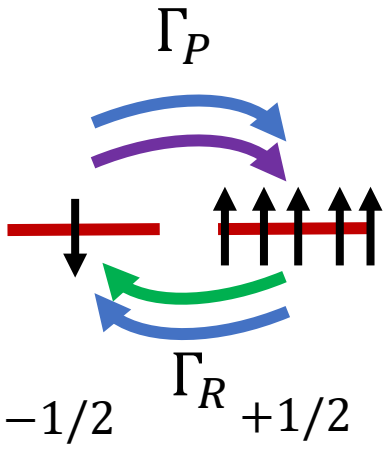

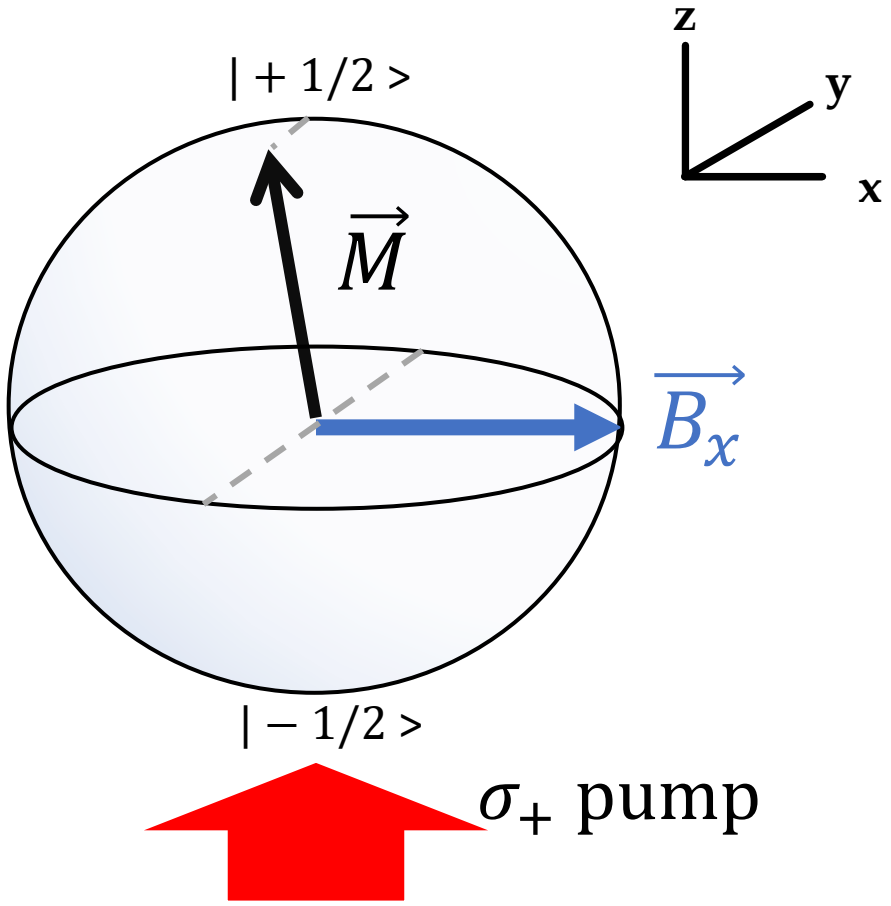

Alkali Magnetometers

- Optically pumped atomic vapors make good magnetometers
- Optical detection of polarized alkali gives **extremely high SNR ~ 10^8**

Magnetic field Measurement error

$$\delta B \approx \frac{1}{\gamma}\sqrt{\frac{\Gamma}{Nt}}$$

Relaxation rate

Number of spins

Gyromagnetic Ratio (Hz/T)

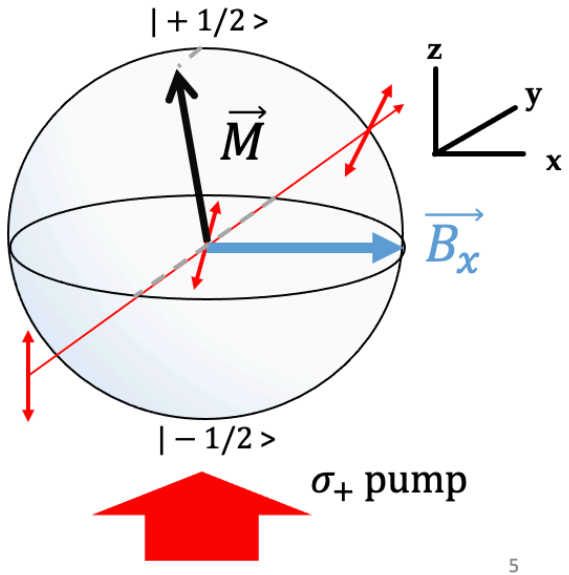

Happer, W., and B. S. Mathur, "Off-resonant light as a probe of optically pumped alkali vapors" *Phys. Rev. Lett.* (1967) DOI:10.1103/PhysRevLett.18.577

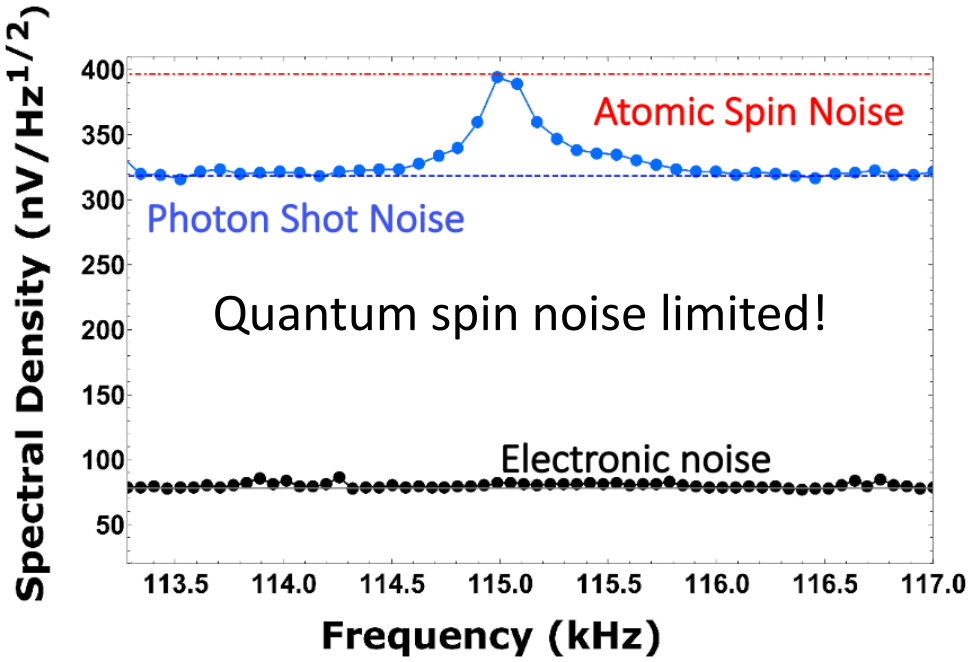

Noble Gas nuclei magnetometers

- Need to work harder to get **extremely high SNR**

Magnetic field Measurement error

$$\delta B \approx \frac{1}{\gamma}\sqrt{\frac{\Gamma}{Nt}}$$

Relaxation rate, long

Number of spins (on order of Avagadro's

Gyromagnetic Ratio (Hz/T)

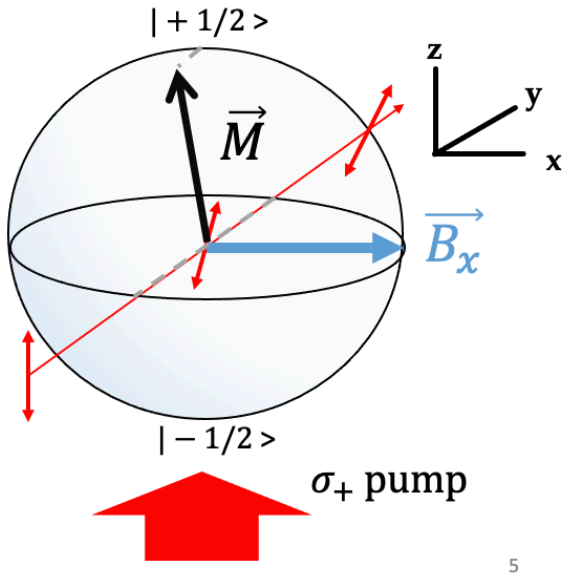

Gas	γ	Relaxation Time
^{3}He	-32.43 MHz/T	Days
^{21}Ne	-3.361 MHz/T	Hours
^{129}Xe	-11.777 MHz/T	Tens of minutes

In principle noble gases can make very good magnetic field measurements < 1 fT/Hz$^{1/2}$, as N and $1/\Gamma$ can be large…
But harder to make quantum-limited measurement

PHYSICAL REVIEW VOLUME 119, NUMBER 2 JULY 15, 1960

Optical Pumping of Helium in the $^3S_1$ Metastable State*†

F. D. COLEGROVE‡ AND P. A. FRANKEN
Harrison M. Randall Laboratory of Physics, The University of Michigan, Ann Arbor, Michigan
(Received March 14, 1960)

- Optically pumped atomic vapors make good magnetometers
- Optical detection of polarized ~~alkali~~ Helium electronic states gives **high SNR**

Magnetic field Measurement error $\delta B \approx \frac{1}{\gamma}\sqrt{\frac{\Gamma}{Nt}}$

Relaxation rate, 1/ 0.1 -10 ms

Number of spins (in metastable state)

Gyromagnetic Ratio (Hz/T)

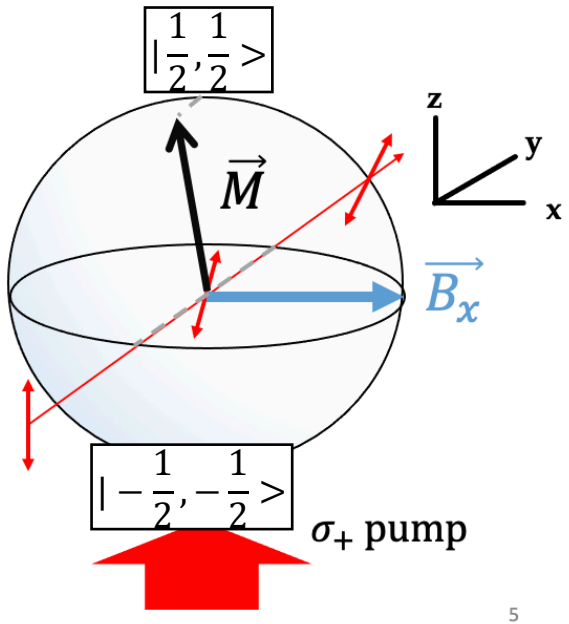

Happer, W., and B. S. Mathur, "Off-resonant light as a probe of optically pumped alkali vapors" *Phys. Rev. Lett.* (1967) DOI:10.1103/PhysRevLett.18.577

$$n^* \approx \frac{\text{Production Rate}}{\Gamma_{diffusion} + \Gamma_{Penning} + \Gamma_{quenching}} \approx 10^9 - 10^{11}\,\frac{atoms}{cc}$$

For ^{4}He, gyromagnetic ratio is close to bare electron, 28.035 GHz/T

Large cell can reach <10 fT/rtHz

Magnetometer Styles

- Near-zero-field, or Resonant magnetometers (RF) are calibrated measurements, i.e. measurement is V -> T , naturally providing vector axes, can use parametric resonances, etc. to extract 3 fields
- Precessing spins in vapor cells naturally provide a scalar measurement, with fundamental calibration is the gyromagnetic ratio $\gamma B \cdot S$ i.e. the measurement is Hz -> T

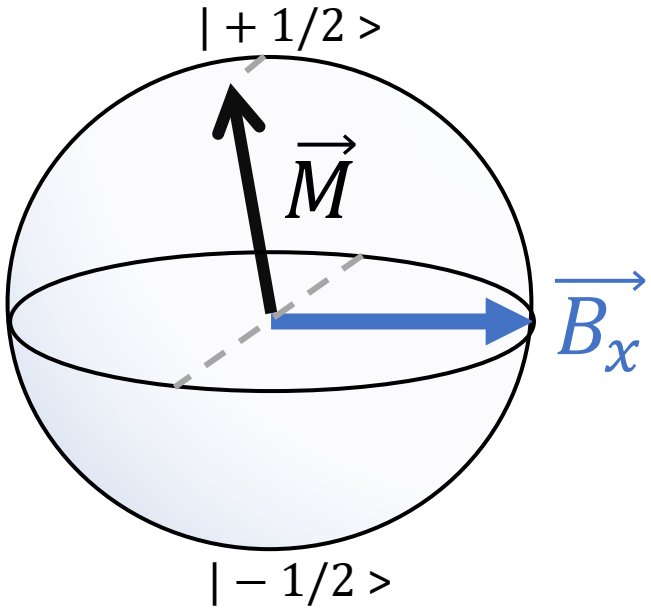

Near-zero-field, can obtain vector info

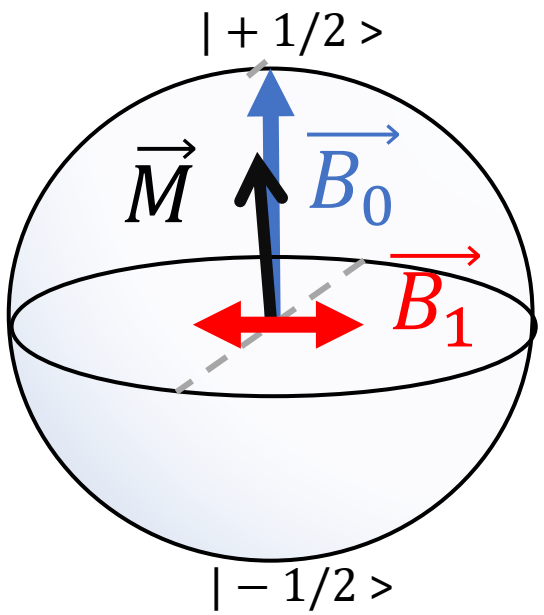

Resonant magnetometer, sensitive to $\omega = \gamma B$ transverse fields (vector axes)

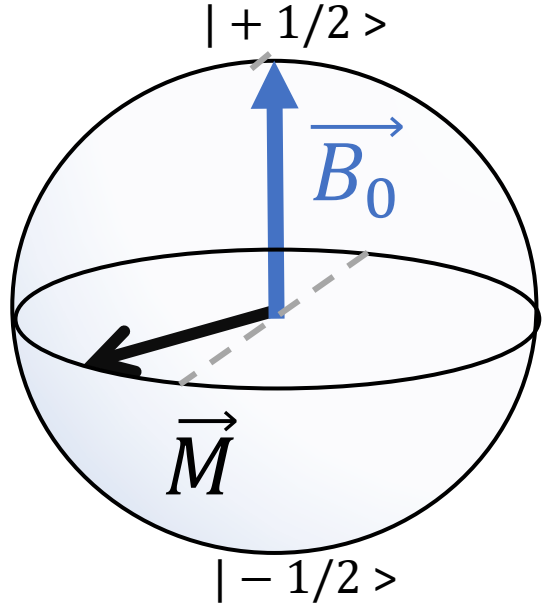

Free-precession about total field
Scalar mag., $\omega = \gamma B$

Scalar free-precession to vector

- Precessing spins in vapor cells naturally provide a scalar measurement, with fundamental calibration is the gyromagnetic ratio $\gamma B \cdot S$ i.e. the measurement is Hz -> T
- Can apply test fields to turn scalar into vector magnetometer

a) jamming on fields B_0 along x, y, z, or

b) smoothly varying test field (variometer)

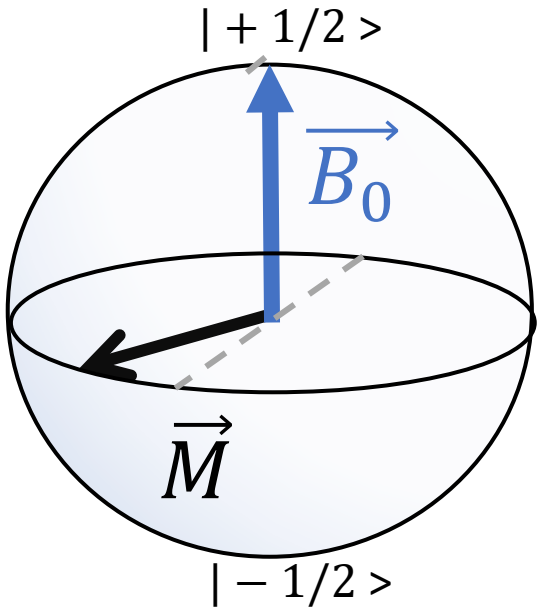

Free-precession about total field
Scalar mag., $\omega = \gamma B$

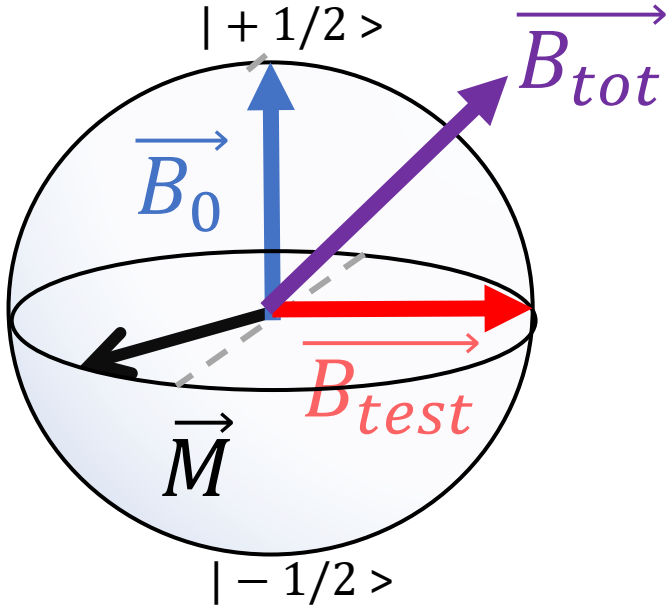

Each shot total $\omega = \gamma B_{tot}$, pulse sequence for $B_{test} \rightarrow x, y, z, -x, -y, -z$ to extract B_x, B_y, B_z (sacrifice bandwidth/sensitivity)

E. Alexandrov, et al., "Three-component variometer based on a scalar potassium sensor" *Meas. Sci. Tech* (2004) DOI: 10.1088/0957-0233/15/5/020

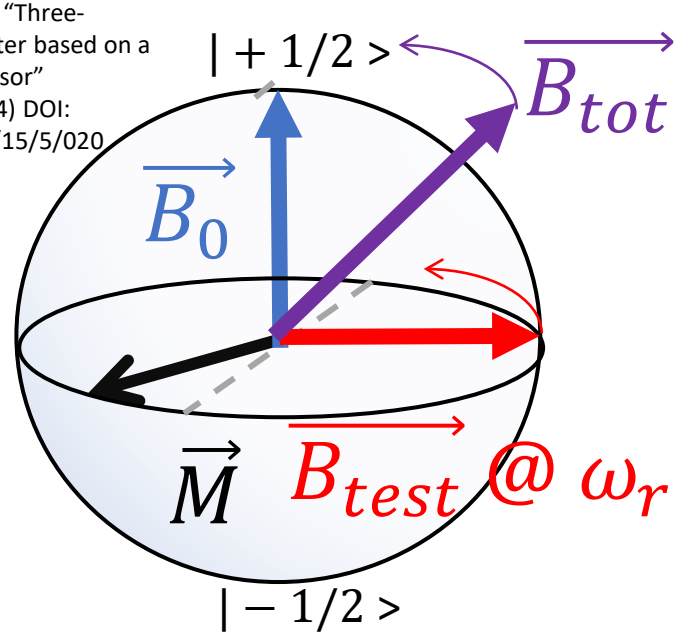

"Variometer", rotate test field at intermediate frequency, lose ~factor x10 sensitivity for transverse axes

Experimental Implementation

- For precision low-ish field magnetometry…

Helps to have a mu-metal shield

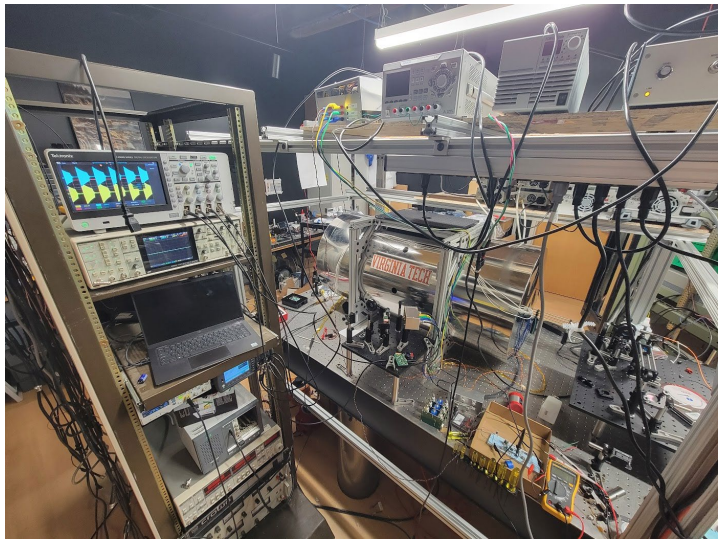

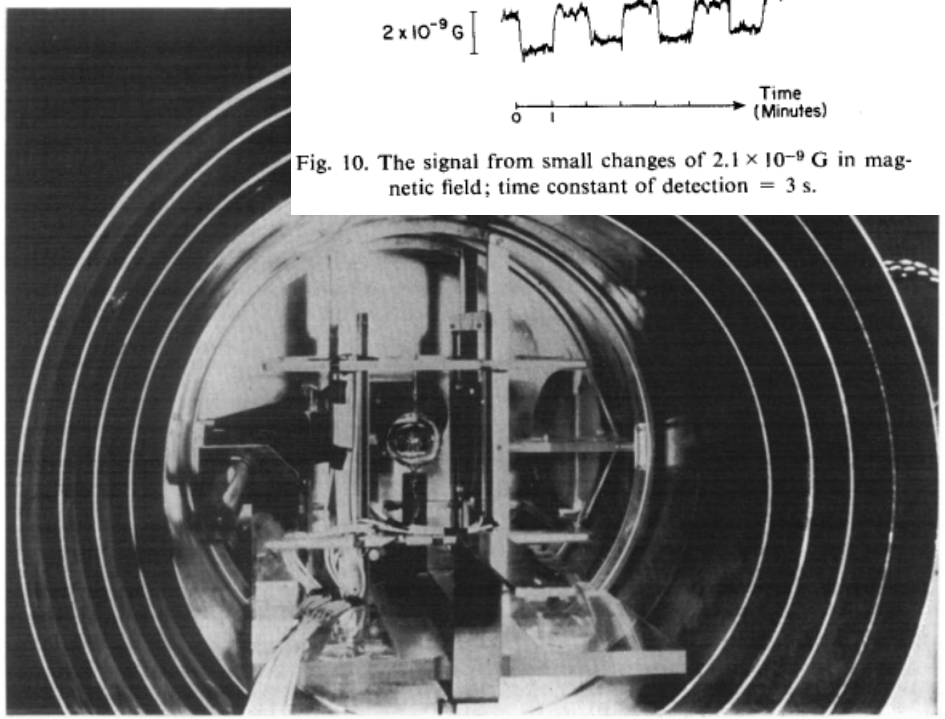

Fig. 10. The signal from small changes of 2.1×10^{-9} G in magnetic field; time constant of detection = 3 s.

Fig. 6. Apparatus used by Cohen-Tannoudji and Haroche for measuring small magnetic fields.

Rule of thumb, you can reach < ~10 fT/rtHz in smallish mu-metal shields (limited by Johnson Noise)

For lower actual magnetic field noise, an inner ferrite cylinder can help get to < ~3 fT/rtHz

For best, superconducting shields

Optical Detection

- Want to be ‘photon shot noise’ limited

Need good light sources, where ‘good’ means sufficient frequency, polarization and amplitude stability

Discharge lamps were the flavor of the day for portable use, until semiconductor lasers became readily available

1.) External cavities can narrow broad semiconductor lasers -> Littrow config, etc

2.) DBR/DFB are edge emitting lasers providing sufficient power for most basic optical pumping experiments

3.) VCSEL lasers are nice, but currently only low powers <1 mW seem to be available commercially for optical pumping wavelengths (telecom is extremely cheap/watt)

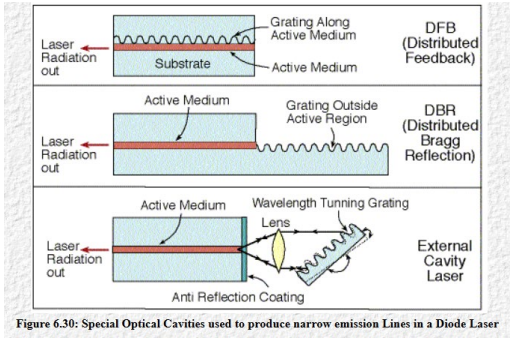

Figure 6.30: Special Optical Cavities used to produce narrow emission Lines in a Diode Laser

Rami Arieli: "The Laser Adventure" Chapter 6.3 Diode Laser, page 17a

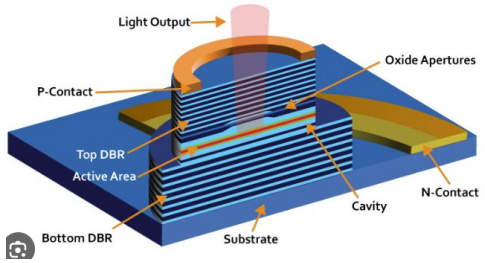

Photodigm

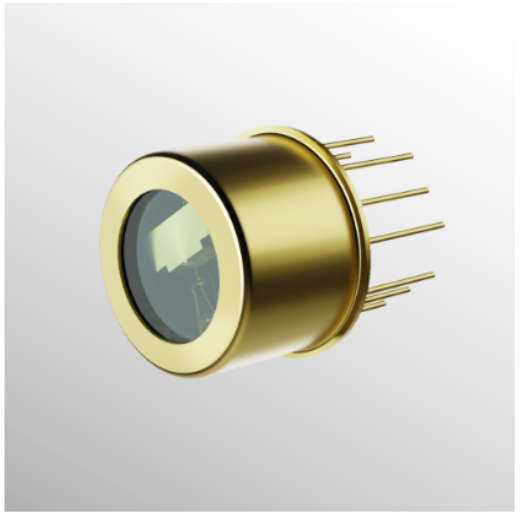

794.978DBRL-T08

Wavelength:	794.978
Chip:	Low Power $1,999
Power:	40 mW – 80 mW
Packaging:	TO-8 $500
Mounting:	Standard

$2,499.00

Optical Detection

- Want to be ‘photon shot noise’ limited

  For sufficiently ‘slow’ applications < 50 MHz, where you have enough light > 0.1 mW, this is pretty straightforward

  Crudely, keep photon shot noise ($\sqrt{2eVR}$, where $P = \frac{V}{R\eta}$, P is power and η is photodiode efficiency) higher than Resistor Johnson noise ($\sqrt{4kTR}$) and op-amp/electronic noise

  Can bias photodiode for faster response

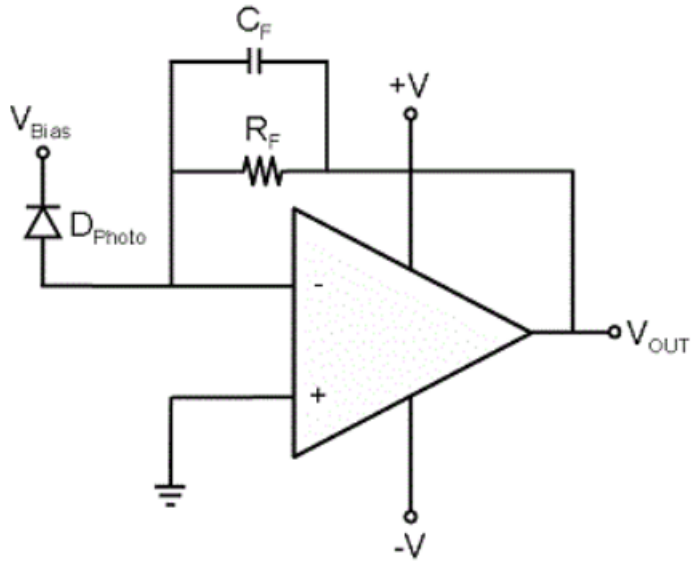

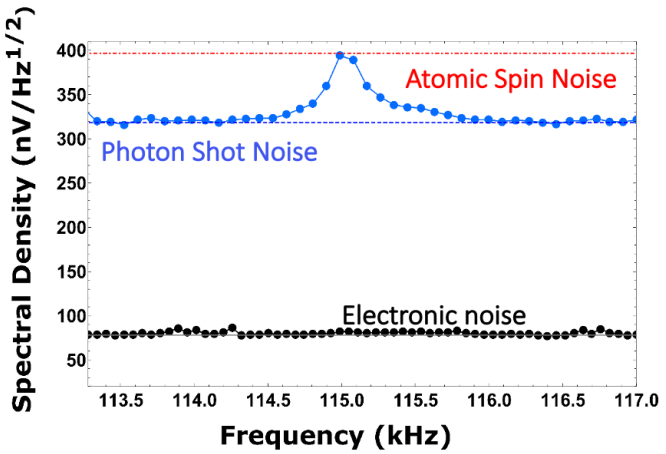

Optical Detection

- Balanced polarimetry of linearly pol. light helps with Amplitude issues

$$\frac{S_s}{S_p} = \frac{\cos^2\phi}{\sin^2\phi}$$

$$\phi = \arctan\sqrt{\frac{S_p}{S_s}}.$$

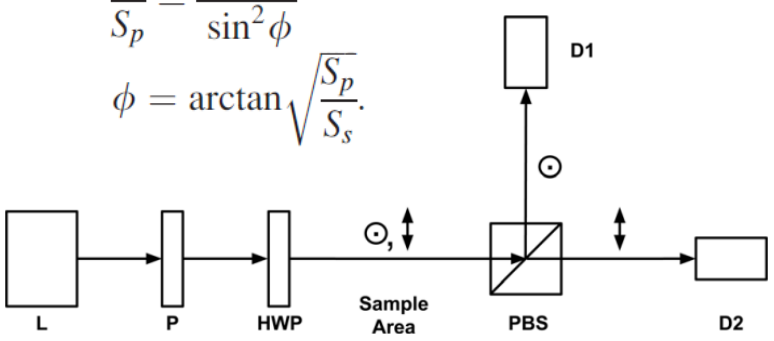

Fig. 1. Schematic of the experimental setup: L is a laser, P is a polarizer, HWP is a half-wave plate (optional), PBS is a polarizing beamsplitter cube, and D1, D2 are light sensors.

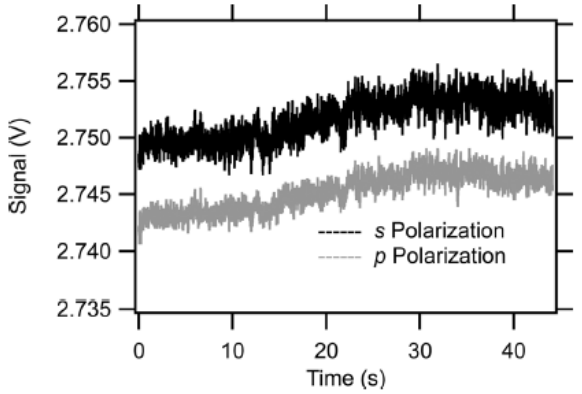

Fig. 2. The smoothed signals from detectors D1 and D2 measured at 1000 Hz during an interval of approximately 45 s with ambient air in the sample compartment.

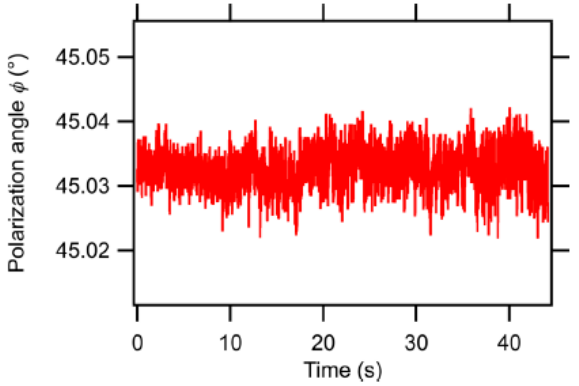

Fig. 3. The smoothed polarization angle, calculated from the data in Fig. 2.

L. Patterson, et al., "Balanced polarimeter: A cost-effective approach for measuring the polarization of light", Am. J. Physics 2015 DOI:10.1119/1.4896747

PDB450A

Switchable Gain Balanced Amp. Photodetector, Si, 320 - 1000 nm

$1,903.40

Light modulation

- Electro-optic modulators,

- Acousto-Optic Modulators,

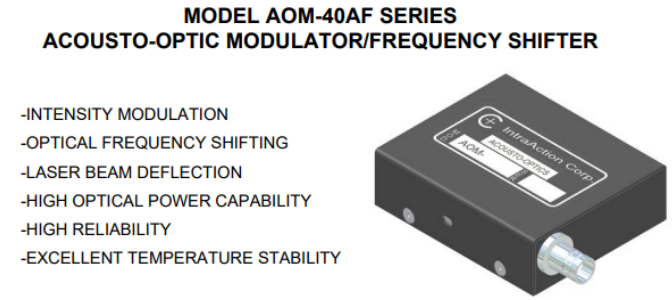

- High Verdet constant crystals +Magnetic field -> Faraday modulator,
-
- Photo-elastic modulators,

- Liquid Crystal Modulators, and more!

can provide phase or amplitude modulation

Main reasons to modulate are
1) Stabilize light conditions (PID)
2) Modulating pump
3) Modulate probe off of 1/f noise

Calibration of magnetometer

- 1) Put in known dummy signal measured by fluxgate, or another trusted magnetometer,

  -> need to make sure calibration is good at test frequency

- 2) Rely on well-known gyromagnetic ratio of alkali or noble gases, etc.

  look at Larmor free precession freq, Rabi freq. for finding coil response at frequency, etc.

Some have magnetometer sensitivity fT/Hz$^{1/2}$ plotted instead of what they actually measured--- a voltage response of their system in V/Hz$^{1/2}$

-> need to divide by frequency dependent calibration curve to get actual sensitivity against frequency

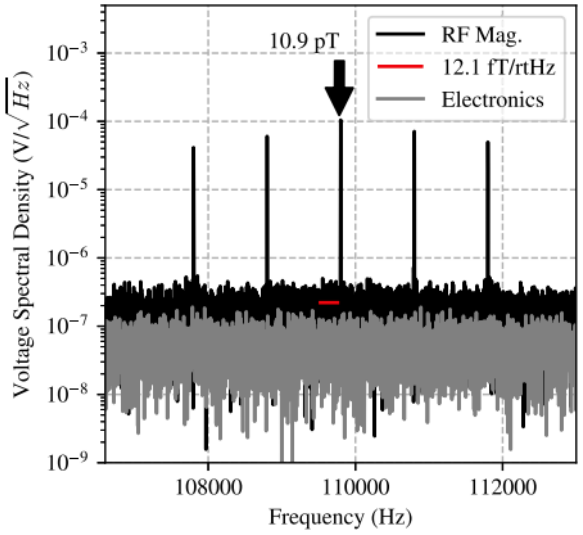

FIG. 4. An RF magnetometer is made with the same geometry as the scalar sensor, where the resonant frequency is determined by the 15.7 μT scalar field strength.

Low-noise electronics

- Want atomic shot noise or photon shot noise to be the ‘weakest link in the chain’
- Need sufficiently low-noise current supplies for magnetic fields, optics analog back-end, heaters for oven, etc. for pure magnetometry, portable or in-shield

Similar requirements in-band for coil or SQUID based NMR detection

- For demonstrations, can project raw magnetometer performance through gradiometry techniques, rejecting things like magnetic field noise from Johnson noise and current supplies

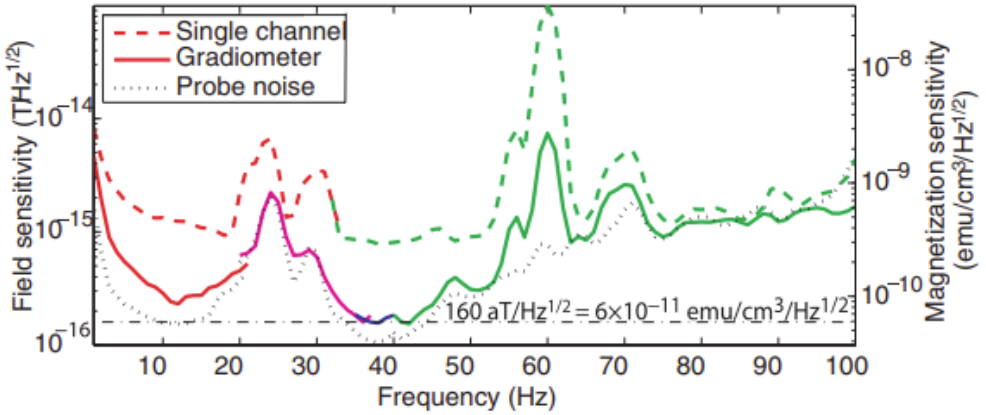

FIG. 3. (Color) Magnetic field response curves (top) and noise spectrum (bottom) for different values of the B_z magnetic field. The left axis shows magnetization sensitivity of the gradiometer.

H. Dang, et al., “Ultrahigh sensitivity magnetic field and magnetization measurements with an atomic magnetometer”, Appl. Phys. Lett. 2010 DOI:10.1063/1.3491215

Sensitivity

- In the standard quantum limit, increasing sensitivity using is a $\frac{1}{\sqrt{Nt}}$ problem ,
- In other words, need N^2 more instantaneous measurements, or t^2 more time for linear gain…
- So it's good to push on sensitivity.
- For noble gases, long-term stability is usually of greater interest-> can characterize through Allan Deviation

$$\sigma_y^2(\tau) = \frac{1}{2(N-1)} \sum_{i=1}^{N-1} (\bar{y}_{i+1} - \bar{y}_i)^2$$

$\boldsymbol{\tau}$: The averaging time (or observation time).

$\boldsymbol{N}$: Total number of data samples.

$\boldsymbol{\bar{y}_i}$: The i-th fractional frequency average over time τ.

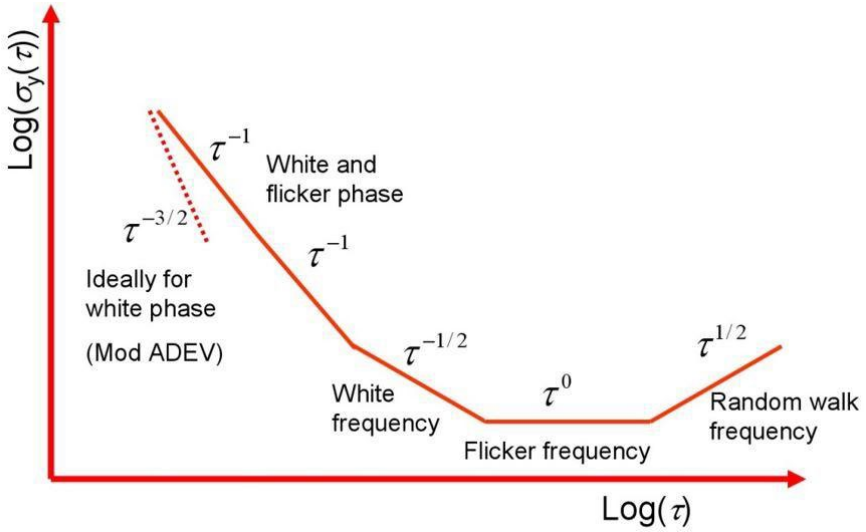

Magnetometry Tutorial

- General Magnetometry 
- Optical Pumping of Metastable Noble gas electronic states (2^3S_1 in ^4He),

  direct optical read-out
- Metastability Exchange Optical Pumping (MEOP) of Noble gas Nuclei,
- Spin Exchange Optical Pumping (SEOP) of Noble gas Nuclei,

  both external read-out via:

  a) coils

  b) SQUIDs or

  c) atoms (can use atoms for in-situ measurements, optically detected)

PHYSICAL REVIEW VOLUME 119, NUMBER 2 JULY 15, 1960

Optical Pumping of Helium in the $^3S_1$ Metastable State*†

F. D. COLEGROVE‡ AND P. A. FRANKEN
Harrison M. Randall Laboratory of Physics, The University of Michigan, Ann Arbor, Michigan

(Received March 14, 1960)

Discharge!

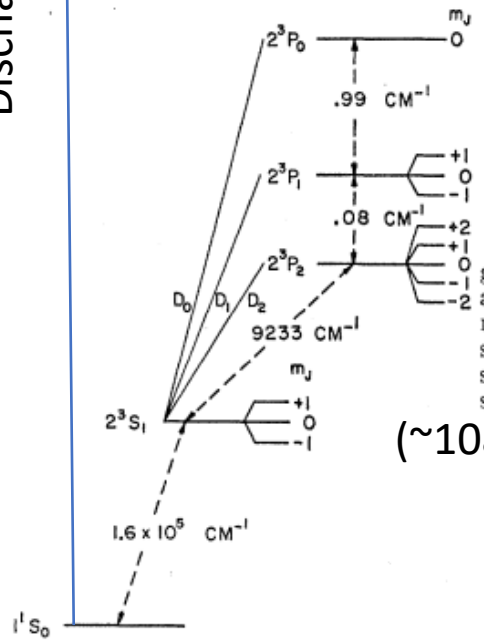

FIG. 2. Relevant energy levels of a helium atom in an external magnetic field (not to scale). The first excited state ($2\,^3S_1$) is metastable.

(~1083 nm)

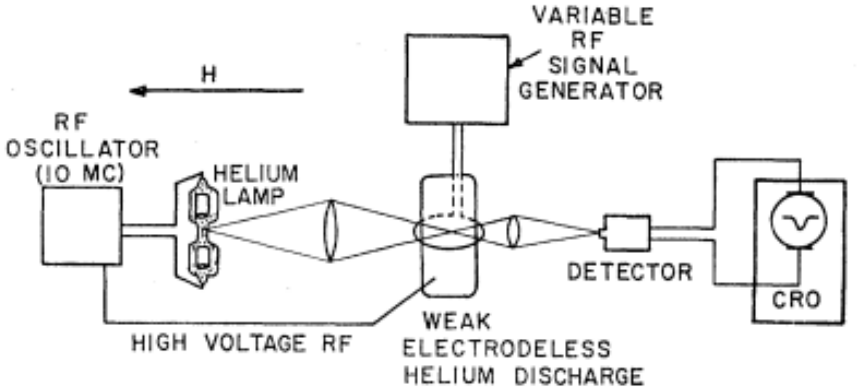

FIG. 1. Schematic diagram of the apparatus.

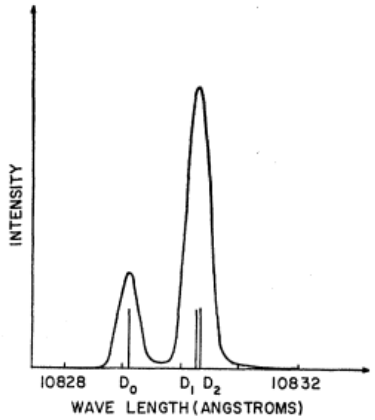

FIG. 4. Spectral profile of the $2\,^3P - 2\,^3S$ helium lines.

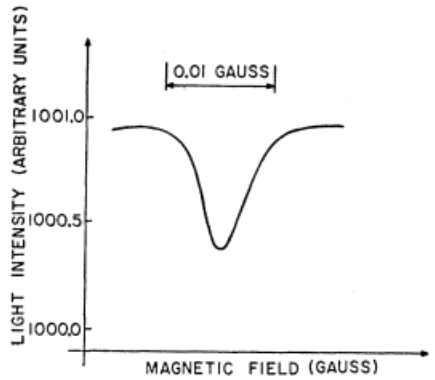

FIG. 3. Resonance signal as displayed on an oscilloscope.

^{4}He magnetometry

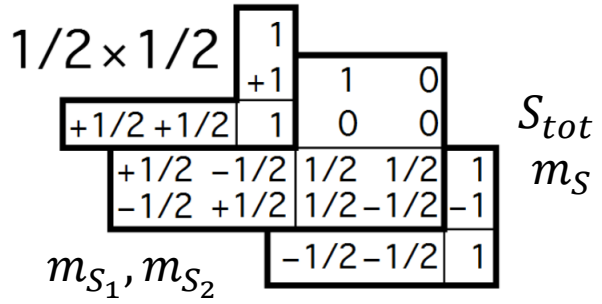

- Add exchange coupling, $J\overrightarrow{S_1}\cdot\overrightarrow{S_2}$, $\frac{1}{2}\otimes\frac{1}{2}=3\oplus 1$
- Triplet singlet basis

$$\sqrt{\frac{1}{2}}\left(\left|\frac{1}{2},-\frac{1}{2}\right>-\left|-\frac{1}{2},\frac{1}{2}\right>\right)$$

$2S_1$ singlet much shorter radiatively (~1-10 ms natural linewidth)

$2S_0$, allows for recombination to $1S_0$

Triplet long naturally long-lived-> 7000 seconds!

$$\left|-\frac{1}{2},-\frac{1}{2}\right> \qquad \sqrt{\frac{1}{2}}\left(\left|\frac{1}{2},-\frac{1}{2}\right>+\left|-\frac{1}{2},\frac{1}{2}\right>\right) \qquad \left|m_{S_1},m_{S_2}\right> \quad \left|\frac{1}{2},\frac{1}{2}\right> \qquad 2S_1$$

$$m_S=-1 \qquad 0 \qquad +1$$

^{4}He magnetometry

- Add Zeeman coupling to strongly coupled states $\gamma\vec{S}\cdot\vec{B}$

$1/2\times1/2$				
	1			
	+1	1	0	
+1/2 +1/2	1	0	0	S_{tot}
+1/2 −1/2		1/2	1/2	1
−1/2 +1/2		1/2	−1/2	−1
		−1/2	−1/2	1
m_{S_1}, m_{S_2}				m_S

High-sensitivity helium resonance magnetometers

Douglas D. McGregor

Texas Instruments, Inc., P. O. Box 660246, Dallas, Texas 75266

(Received 10 September 1986; accepted for publication 4 March 1987)

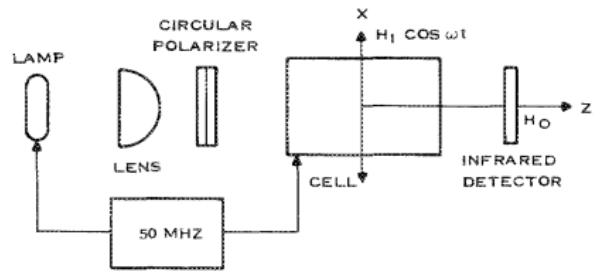

$$\left|-\frac{1}{2},-\frac{1}{2}\right> \rightarrow -\gamma B_0$$

$$\sqrt{\frac{1}{2}}\left(\left|\frac{1}{2},-\frac{1}{2}\right> + \left|-\frac{1}{2},\frac{1}{2}\right>\right) \rightarrow 0$$

$$\left|\frac{1}{2},\frac{1}{2}\right> \rightarrow \gamma B_0$$

$m_S = -1$ 0 $+1$

Two electronic spin states coupled result in a 'effective γ' of something close to gyromagnetic ratio, 28.035 GHz/T

i.e. Earth-scale field of 50 μT gives a resonance freq. of 1.4 MHz.

^{4}He magnetometry

- Optical Pumping $L + S$, (P orbital has L = 1, S = 1)

Depopulate states, with linear or circularly polarized light

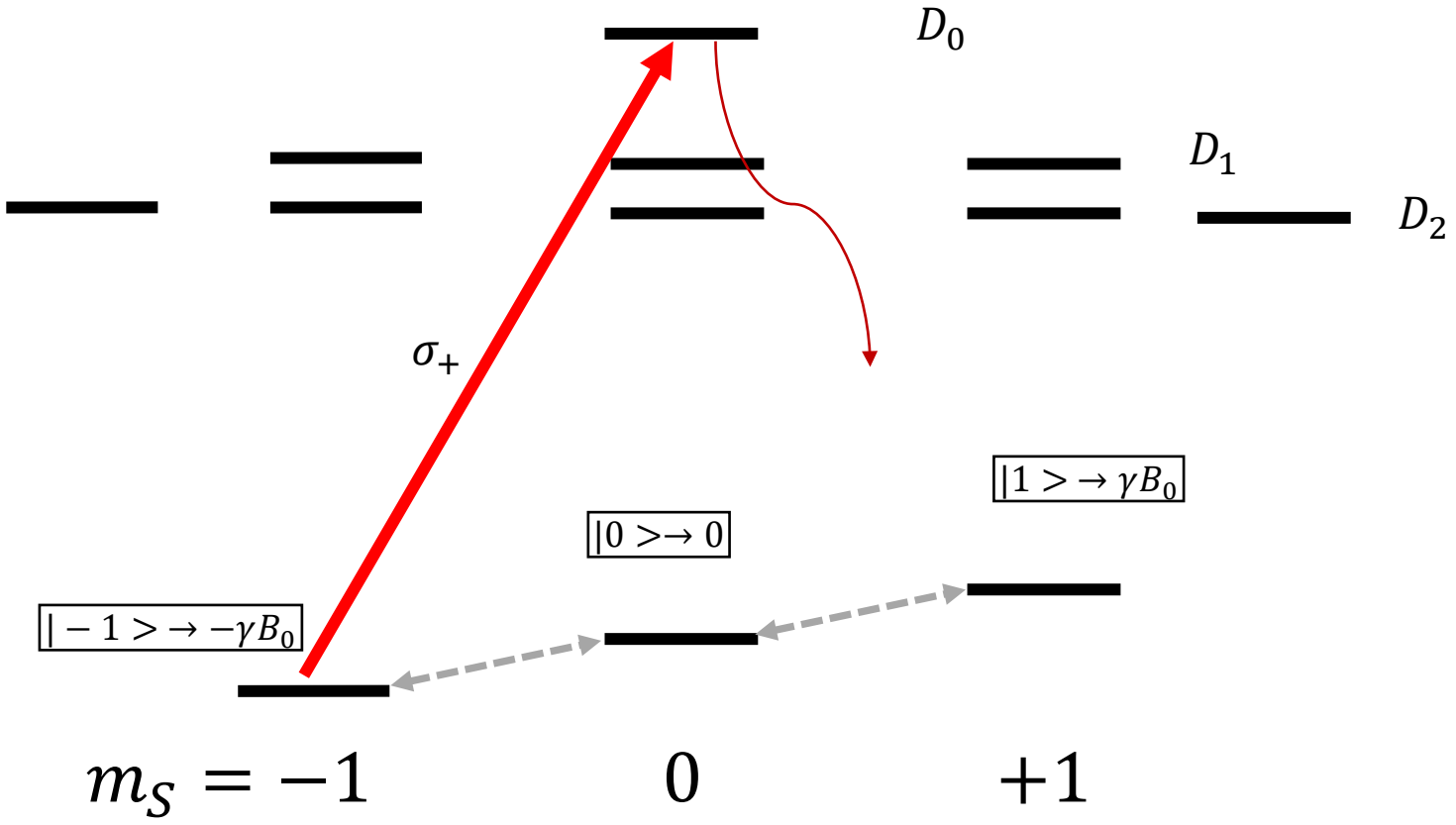

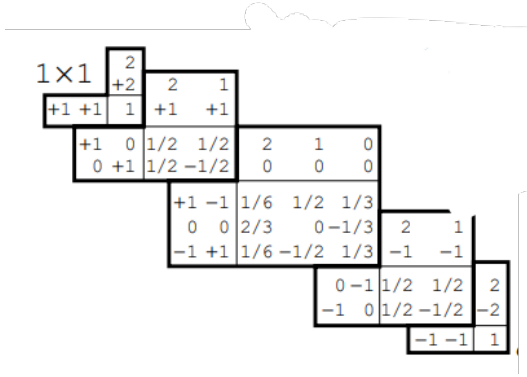

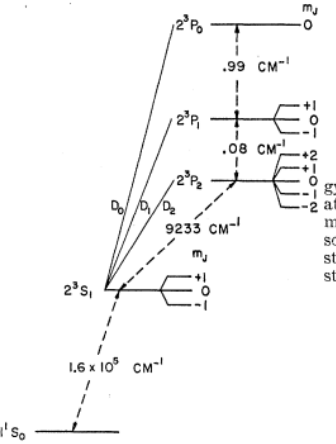

FIG. 2. Relevant energy levels of a helium atom in an external magnetic field (not to scale). The first excited state ($2\,^3S_1$) is metastable.

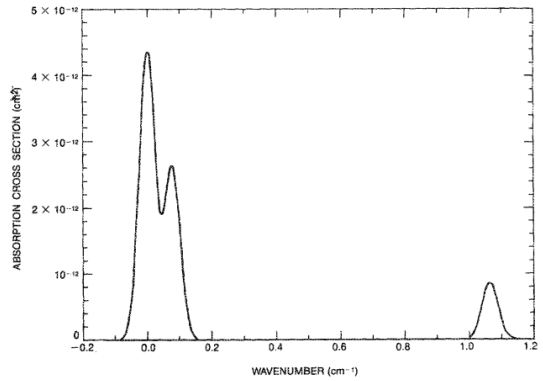

FIG. 2. The absorption cross section for 2^3S_1 He^4 at 300 K vs wavenumber. The indicated wavenumber is referenced to 9230.8 cm^{-1}.

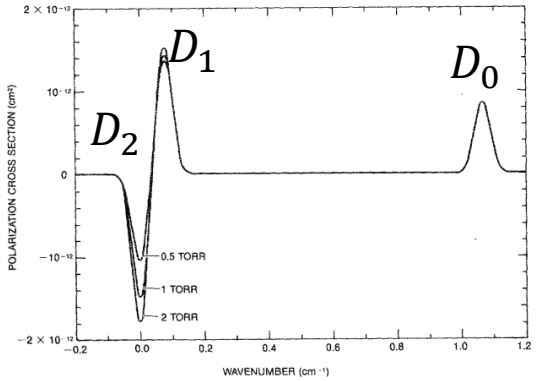

FIG. 3. The polarization cross section for 2^3S_1 He^4 at 300 K vs wavenumber (relative to 9230.8 cm^{-1}). Curves are shown for pressures of 0.5, 1, and 2 Torr. The pumping beam is left circularly polarized.

^{4}He magnetometry

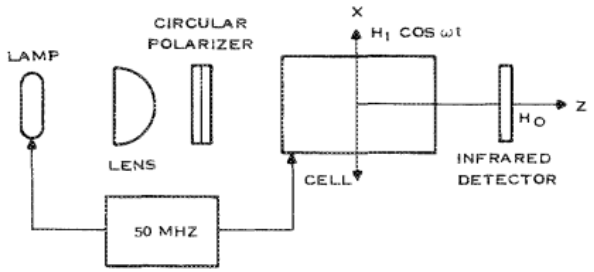

- 1) Depopulate, transmission reaches a steady state on photodiode

(No population, no absorption)

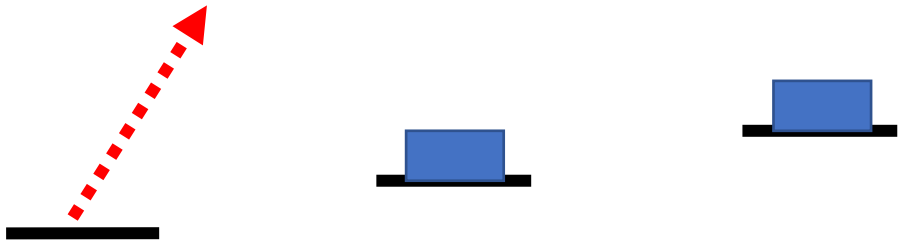

$m_S = -1$ $\quad 0 \quad +1$

2) Apply transverse resonance, transmission dips

(States absorb light)

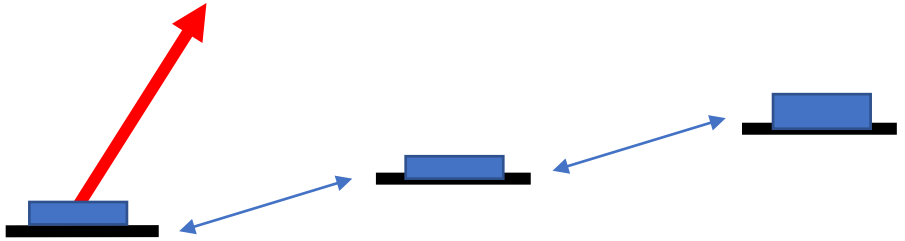

$m_S = -1$ 1.4 MHz $0 \quad +1$

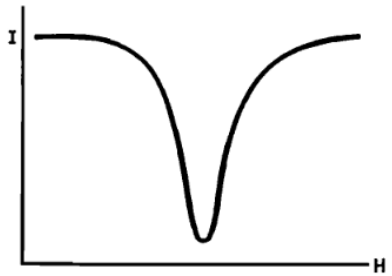

Fig. 1. Resonance signal.

Can lock to resonance line a variety of ways

^{4}He magnetometry

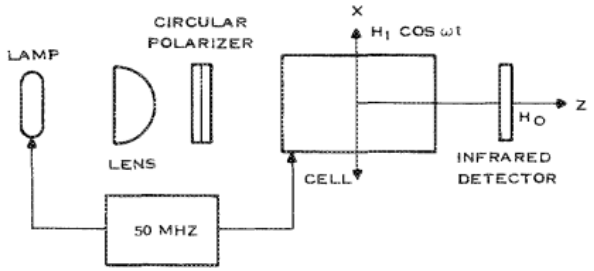

1960's Colegrove + Franken at U. of Michigan -> Sold to Texas Instruments… "1500 scalar 4He mags for submarine detection"
Made vector mag for space use
Used in Vietnam, etc. for magnetic anomaly detection

Recent include Polatomic Inc. backed by US Navy, and CEA-Leti for SWARM satellites

POLATOMIC

cea leti

esa swarm

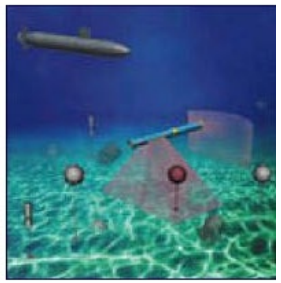

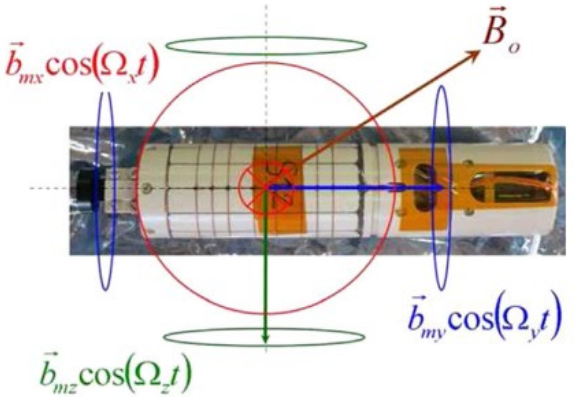

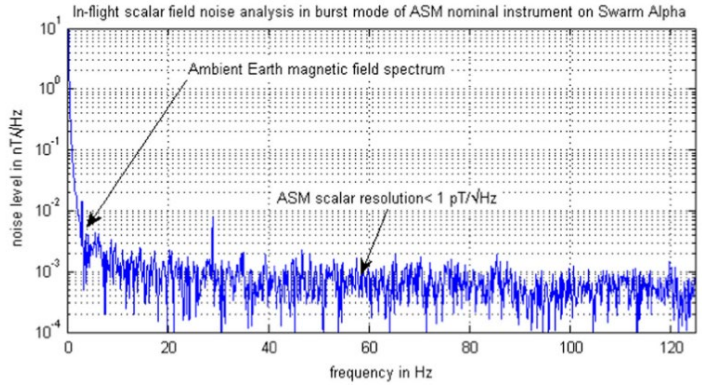

^{4}He magnetometry

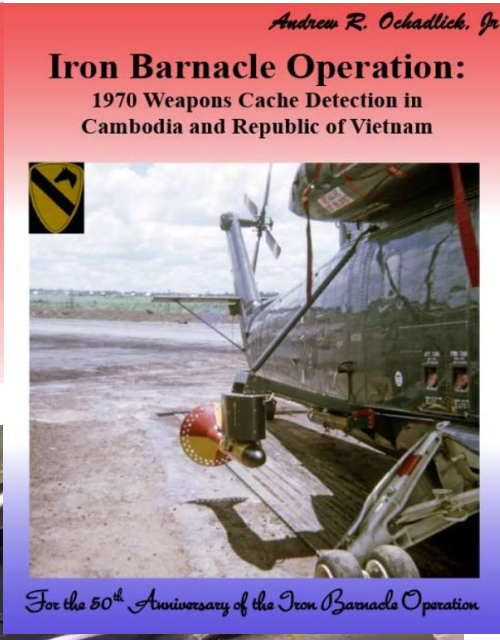

LDM #257: Magnetic Anomaly Detector AN/ASQ-81(V) - Part 1: Teardown

Le labo de Michel
48.2K subscribers
Subscribe

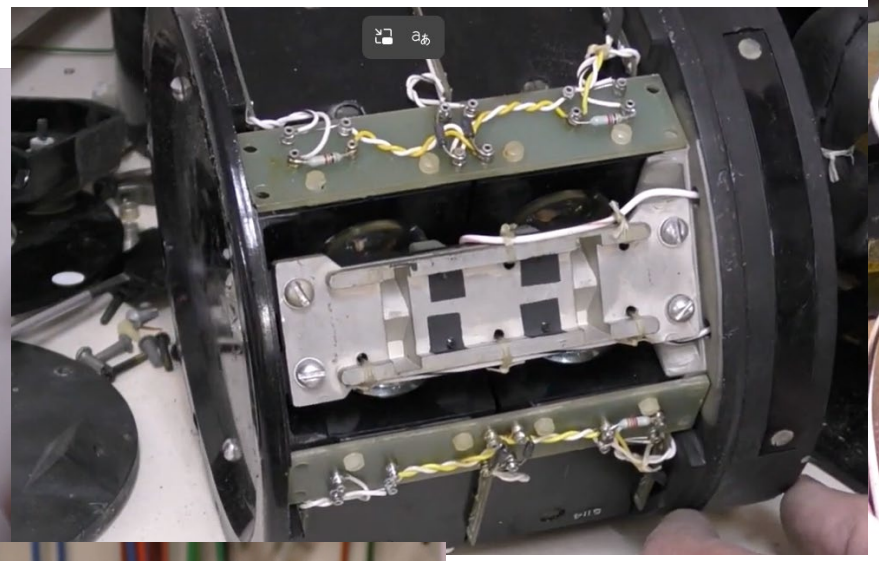

Some screws are missing here.

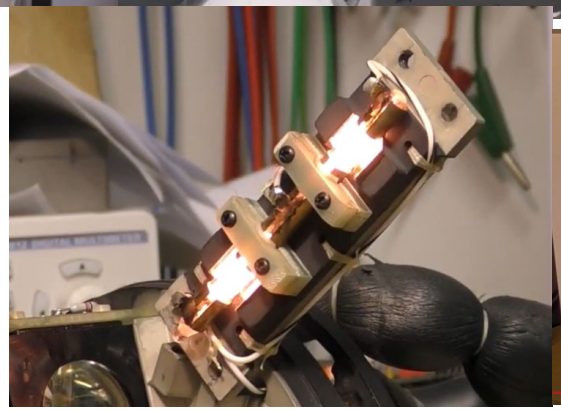

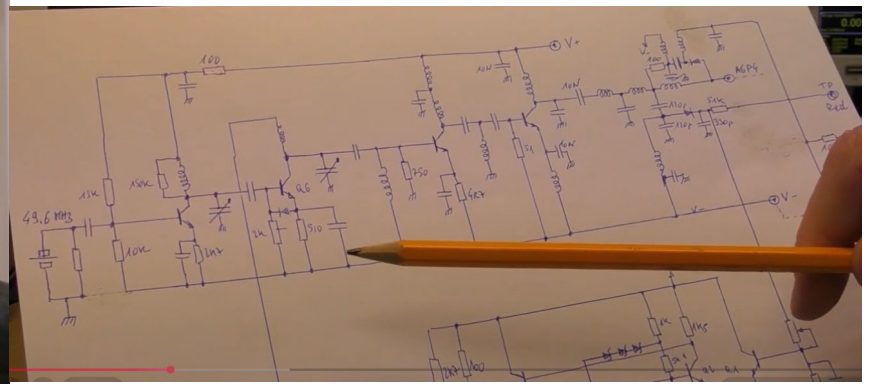

New ^{4}He mag.

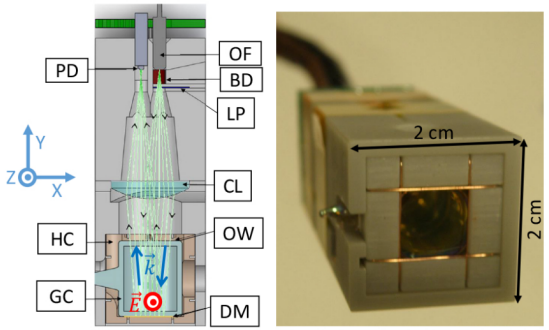

Fig. 1. Helium-4 compact OPM. (a) Cross-section showing the functional parts. (b) Photograph showing the bottom of the sensor and its footprint size. LP: linear polarizer. OF: optical fiber. PD: InGaAs photodiode. CL: converging lens. OW: optical window. DM: dielectric mirror. GC: glass cell containing helium-4. HC: triaxial Helmholtz coils. BD: beam divergence.

W. Fourcault, et al., "Helium-4 magnetometers for room-temperature biomedical imaging: toward collective operation and photon-noise limited sensitivity", Optics Express, 2021
DOI:10.1364/OE.420031

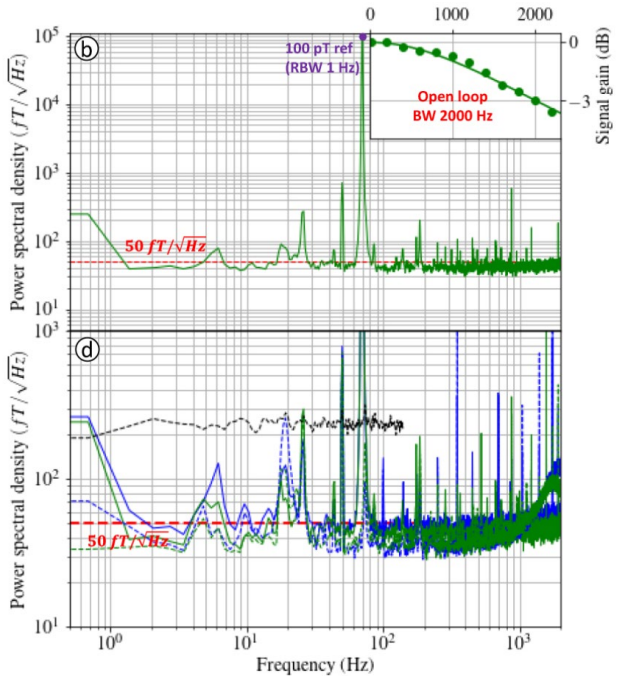

50 fT/Hz$^{1/2}$ Physiologically relevant sensitivities

New ^{4}He mag.-multipass

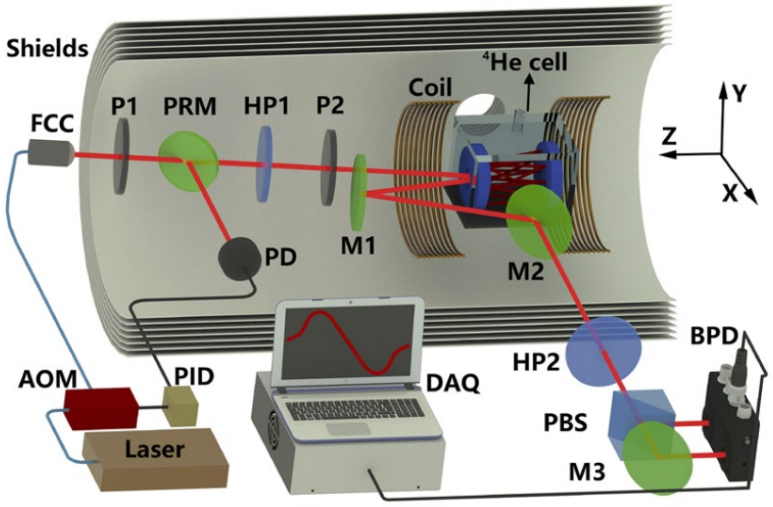

Y. Liu, et al., "Femtotesla 4He magnetometer with a multipass cell",Optics letters, 2022 DOI:10.1364/OE.471557

<10 fT/rtHz! "Zero field" operation in this paper

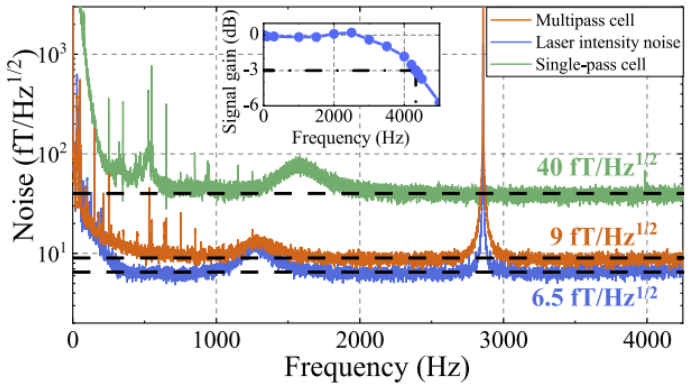

Fig. 3. Noise spectral density (NSD) and frequency response (or bandwidth) of the NMOR ^{4}He magnetometer. The orange curve is the NSD of magnetic measurement, with a noise floor of 9 fT/Hz$^{1/2}$; the blue curve is the NSD from laser intensity noise measured with no RF discharge and the same input optical power to the balanced photodetector, with a noise floor of 6.5 fT/Hz$^{1/2}$; the green curve is the NSD of the same scheme with a single-pass cell, with a noise floor of 40 fT/Hz$^{1/2}$. The inset shows the frequency response of the NMOR ^{4}He magnetometer measured with a 20 nT$_{pp}$ sinusoidal magnetic field.

M. A. Bouchiat, Pottier, "Light-Polarization Modifications in a Multipass Cavity", Applied Physics B, 1982 DOI:10.1103/10.1007/BF00694368

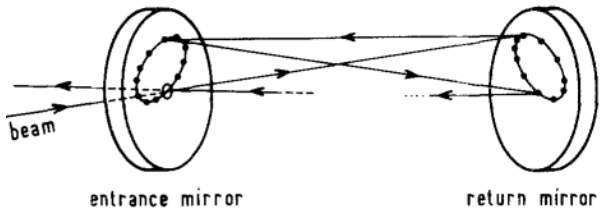

Fig. 1. The multipass (not all passes are represented)

Gist of multipass---non-resonant optical cavity -> Think "Herriot cell" for gas spectroscopy, developed for alkali magnetometry by Romalis

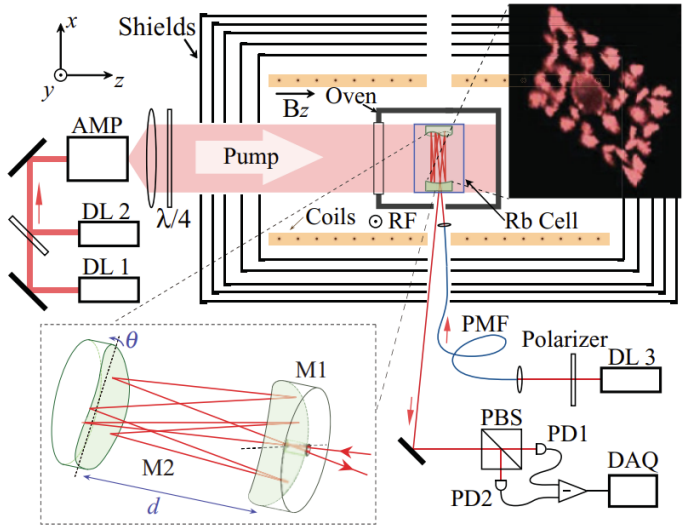

$$\phi_0 = \tfrac{1}{2} n l r_e c P f / (\nu - \nu_0)$$

Getting increased optical rotation while keeping photon shot noise the same

S. Li, et al., "Optical rotation in excess of 100 rad generated by Rb vapor in a multipass cell", PRA, 201 DOI:10.1103/PhysRevA.84.061403
D. Sheng, et al., "Subfemtotesla Scalar Atomic Magnetometry Using Multipass Cells", PRL, 201 DOI:10.1103/PhysRevLett.110.160802

Magnetometry Tutorial

- General Magnetometry
- Optical Pumping of Metastable Noble gas electronic states (2^3S_1 in ^4He),

  direct optical read-out
- Metastability Exchange Optical Pumping (MEOP) of Noble gas Nuclei,
- Spin Exchange Optical Pumping (SEOP) of Noble gas Nuclei,

  both external read-out via:

  a) coils

  b) SQUIDs or

  c) atoms (can use atoms for in-situ measurements, optically detected)

Polarization of He^3 Gas by Optical Pumping

F. D. COLEGROVE, L. D. SCHEARER,* AND G. K. WALTERS*
Texas Instruments Incorporated, Dallas, Texas
(Received 5 August 1963)

The process of He^3 nuclear polarization by metastability exchange with optically pumped metastable He^3 atoms is described and experimental details given. Phenomenological theories are presented which explain the optical signals and the time variation of the polarization. The polarization is measured both optically and by nuclear magnetic resonance. Relaxation of the nuclear spins by diffusion through magnetic field gradients is discussed. When gradients are small, nuclear relaxation times as long as 4000 sec have been measured. The maximum polarization achieved was 40±5% in He^3 gas at a pressure of one mm Hg.

Coupling the metastable and ground-state magnetic sublevels are collisions involving metastability exchange,

$$He^3 + He^{3*} \rightarrow He^{3*} + He^3,$$

where * denotes an atom in the $^3S_1$ metastable state.

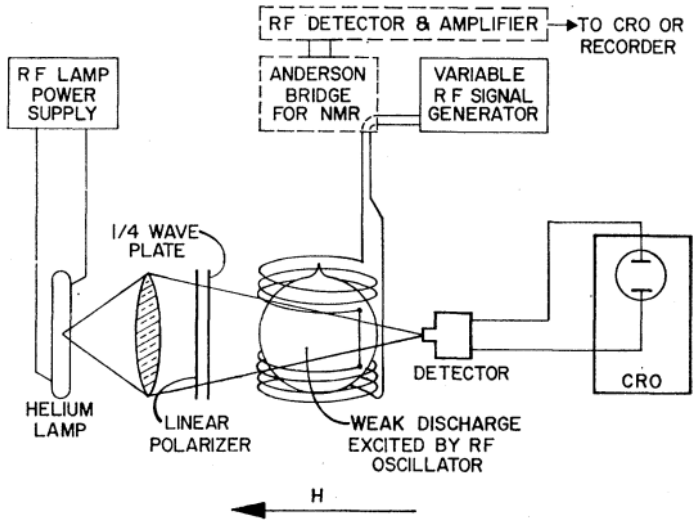

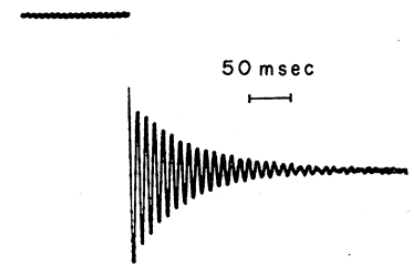

FIG. 9. Change in transmitted light upon sudden application of oscillating magnetic field at nuclear Larmor frequency.

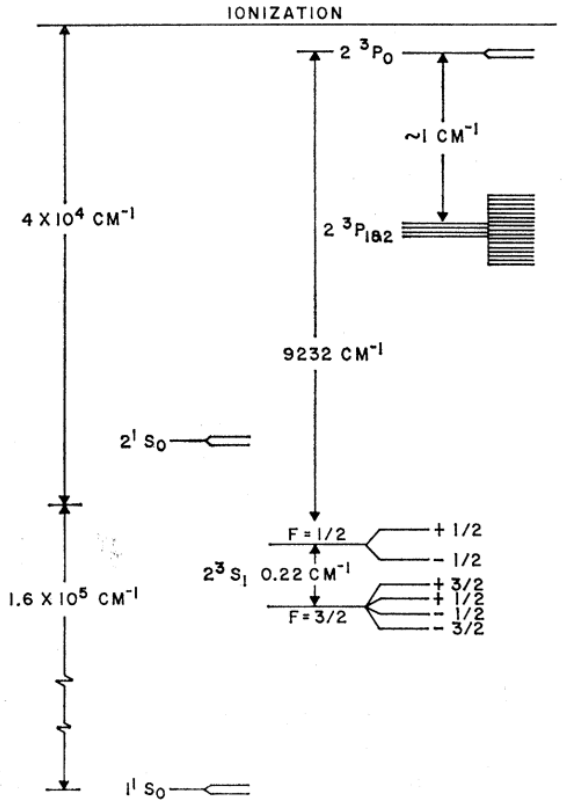

FIG. 1. Energy levels of He^3 atom in external magnetic field (not to scale).

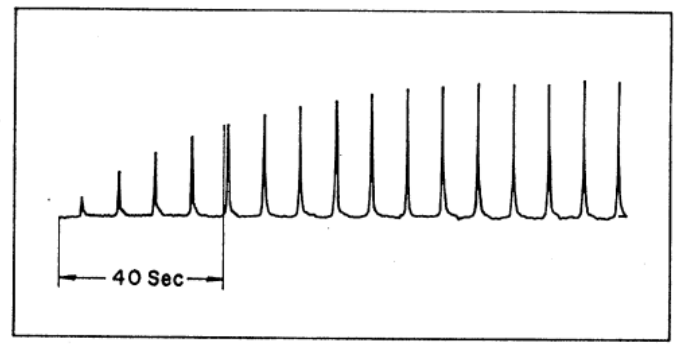

FIG. 10. Growth of precessing macroscopic moment in "crossed-beam" experiment shown by successive passes through resonance.

^{3}He magnetometry

- Optical Pumping $L + J$, (P orbital has L = 1, J = 3/2, 1/2)

Depopulate states, with linear or circularly polarized light

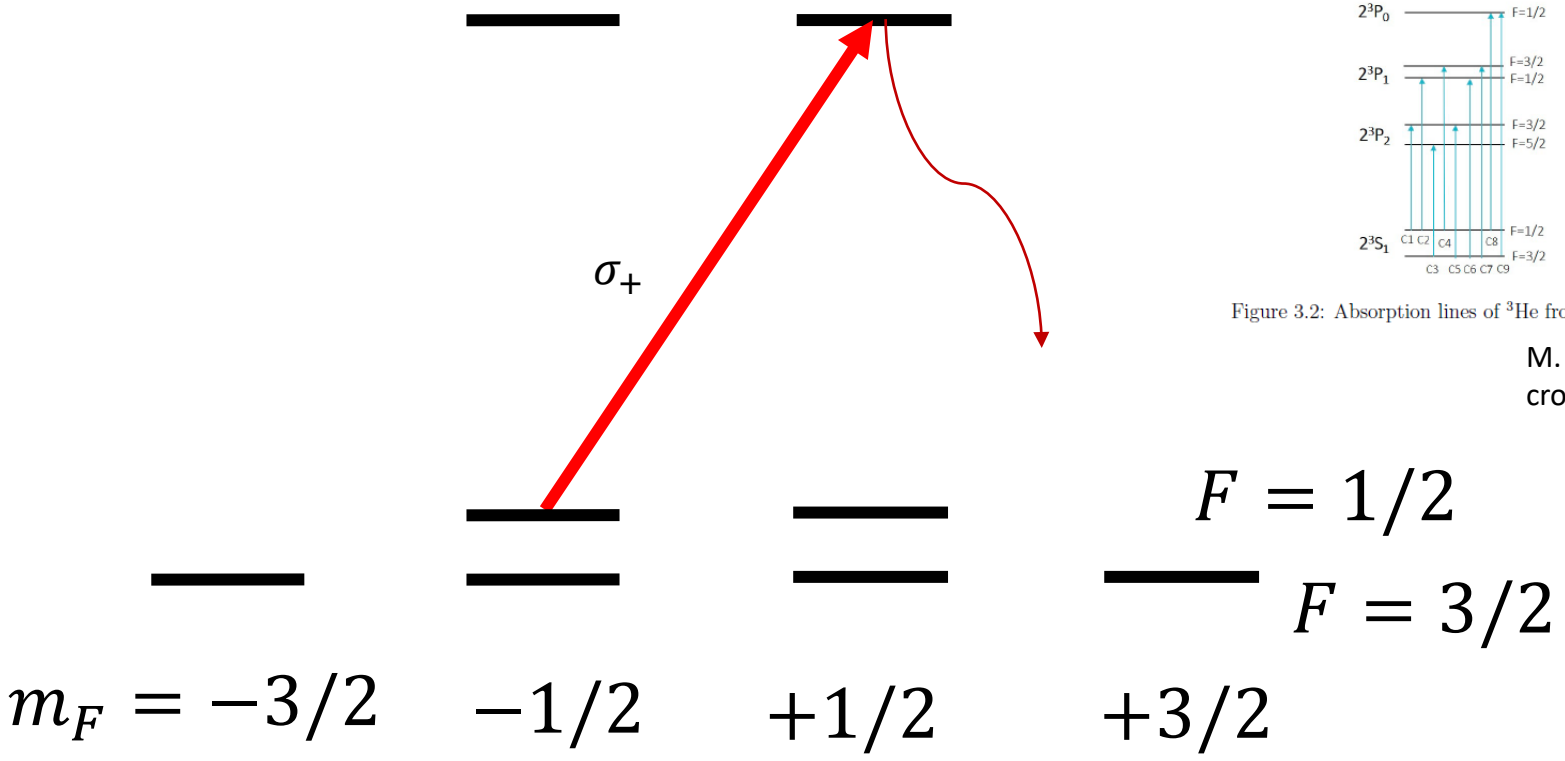

Figure 3.2: Absorption lines of ^{3}He from 2^3S to 2^3P

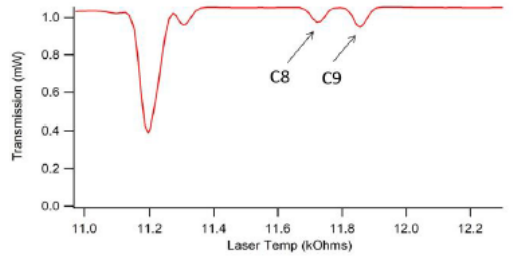

Figure 4.4: Measured ^{3}He absorption spectrum at low field.

M. Farooq, "Absolute magnetometry with 3He:
cross calibration with protons in water", Dissertation 2019

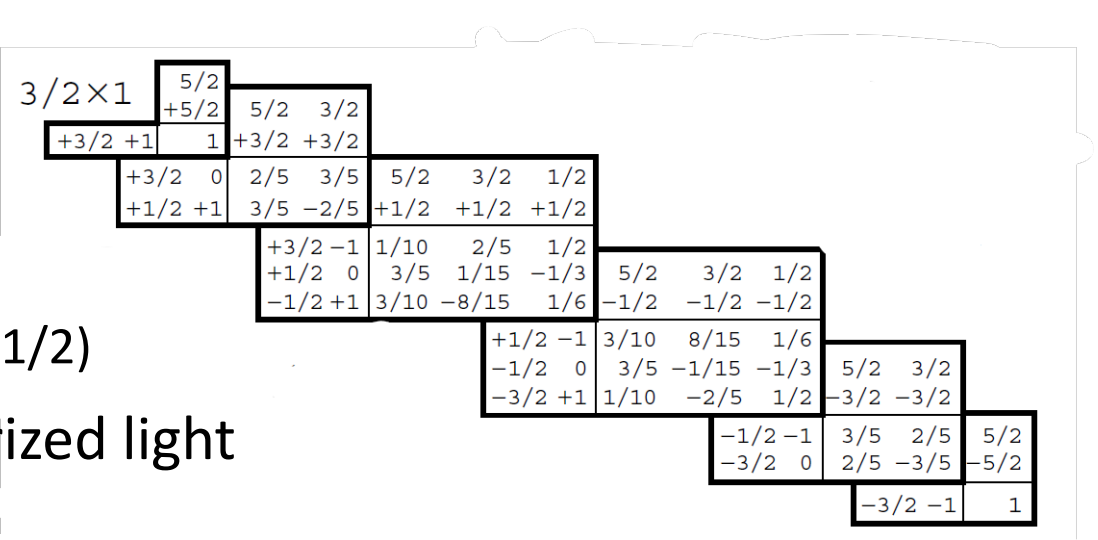

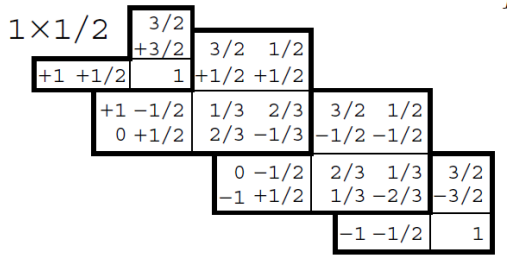

MEOP ^{3}He detected by coil

- Example: F. Colegrove, et al., “HE3 SOLENOID MAGNETOMETER”, Canadian patent, 2,049,148 1991

1.) Spark discharge
2.) Metastability Exchange Optically Pump ground state ^{3}He noble gas nuclei (pumping on order of 10s of seconds to minutes)
3.) Shut off discharge
4.) Tip spins
5.) Detect free precession in earth’s field with coil

3He Gyromagnetic ratio is -32.43 MHz/T
Earth’s field 50 μT $\rightarrow$ 1.621 kHz… low freq…
High-turn detection coil
Be careful of radiation damping

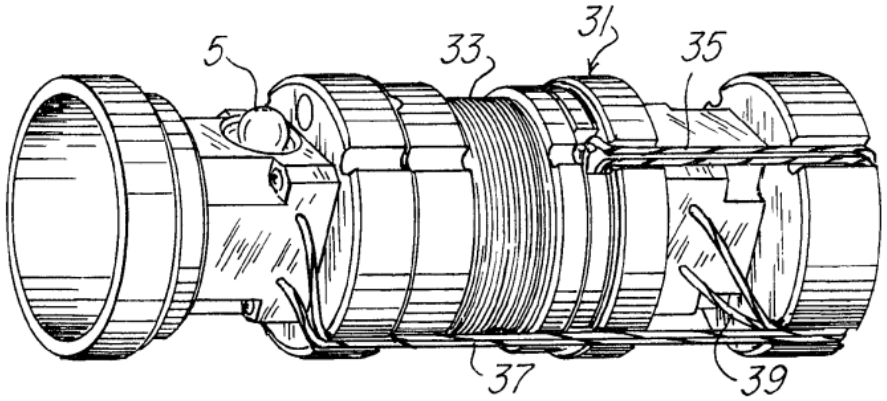

“The frequency of the signal from pick-up coil (33) is a direct and precise measurement of the magnetic field surrounding the sensor”

Can also be done with ‘high-field’ NMR

Example: M. Farooq, et al., “Absolute Magnetometry with ^{3}He” , PRL, 2020, DOI:10.1103/PhysRevLett.124.223001

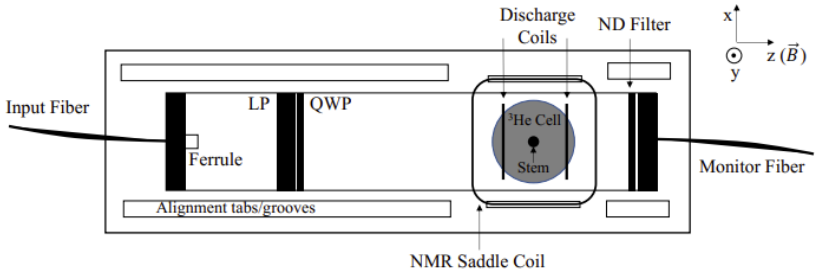

Coil v. atomic sensitivity

I. M. Savukov , Seltzer, M. V. Romalis, “Detection of NMR signals with a radio-frequency atomic magnetometer”, JMR, 2012 , DOI:10.1016/j.jmr.2006.12.012

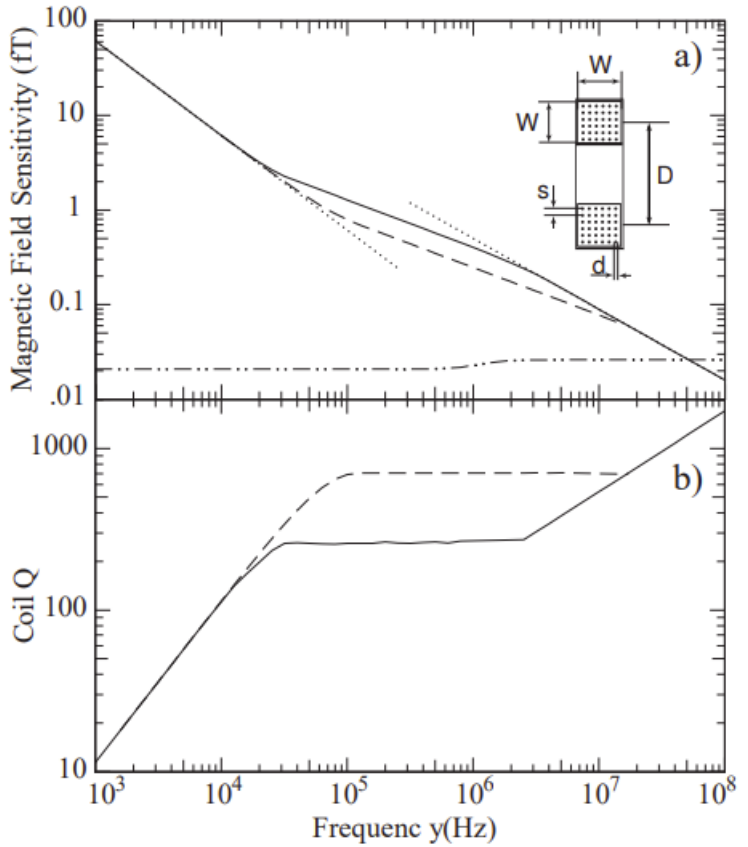

FIG. 6: Panel a) Estimated optimal magnetic field sensitivity for a surface pick-up coil with dimensions $D = 5$ cm and $W = 1$ cm. Solid curve gives the sensitivity for solid wire, while dashed curve is for Litz wire with 1000 strands. The total number of turns and the diameter of the wire is optimized at each frequency. Dotted lines show the asymptotic sensitivity of the coil at low frequency from Eq. (2) and high frequency from Eq. (8). Dot-dashed line shows sensitivity for a K atomic magnetometer occupying the same volume as the coil. Panel b) The Q of the coil with parameters that give optimal sensitivity in panel a). Solid line is for solid wire, dashed line for Litz wire

MEOP ^{3}He detected optically

- Y. Lu, et al., "^{3}He absolute magnetometer at geomagnetic field", Phys. Rev. Research, 2025, DOI:10.1103/dx7x-wdqv

  1.) Spark discharge
  2.) Metastability Exchange Optically Pump ground state ^{3}He noble gas nuclei (pumping on order of 10s of seconds to minutes)
  4.) Tip spins
  5.) Detect free precession optically

  4.8 pT/Hz$^{1/2}$ at 50 μT
  0.18 pT/Hz$^{1/2}$ at 10 μT

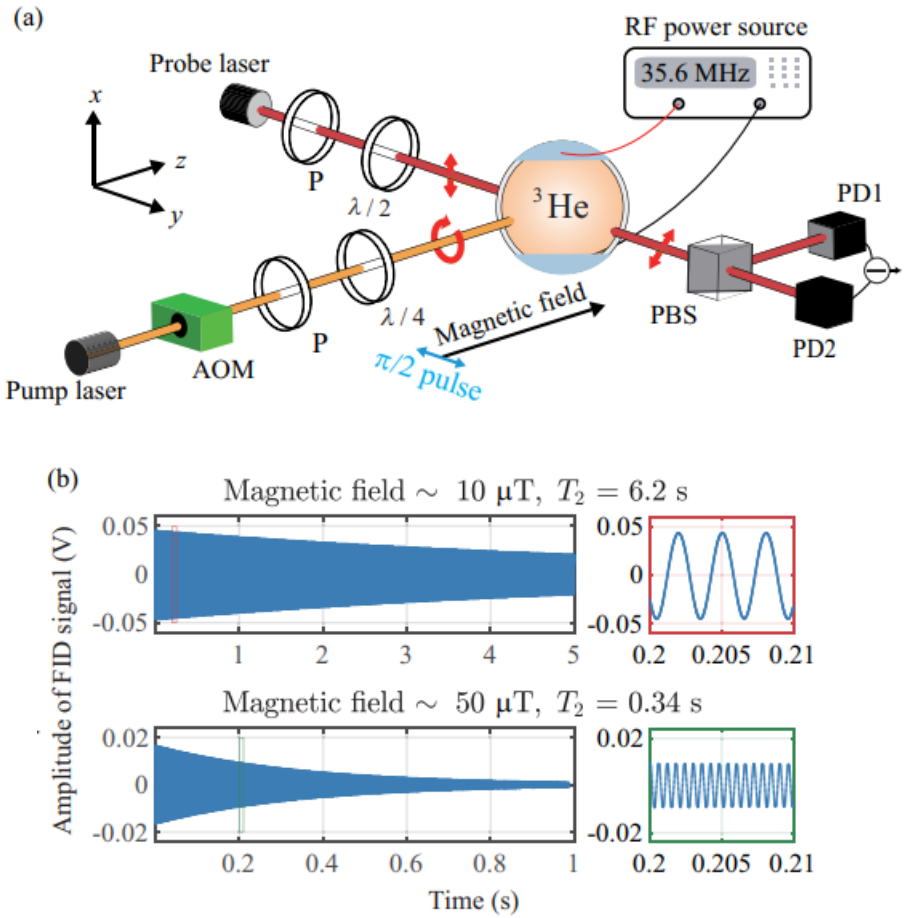

DETECTION OF THE STATIC MAGNETIC FIELD PRODUCED BY THE ORIENTED NUCLEI OF OPTICALLY PUMPED ^{3}He GAS

C. Cohen-Tannoudji, J. DuPont-Roc, S. Haroche, and F. Laloë
Faculté des Sciences, Laboratoire de Spectroscopie hertzienne de l'Ecole Normale Supérieure, associé au Centre National de la Recherche Scentifique, Paris, France
(Received 10 March 1969)

A new type of very sensitive low-field magnetometer is used to detect the static magnetic field produced by optically pumped ^{3}He nuclei in a vapor. Various signals (pumping and relaxation transients) are obtained in this way. This magnetostatic detection allows a direct study of ^{3}He nuclear polarization without perturbing the spins.

The experimental setup is shown schematically in Fig. 1. A 6-cm-diam cell contains the ^{3}He nuclei; the magnetic field they produce is detected by ^{87}Rb atoms contained in the second cell. Both cells are placed in a magnetic shield which considerably reduces (by a factor 10^5) the external magnetic noise, much larger than ΔH. The shield also lessens considerably the magnetic field inhomogeneities, so that we can observe, as we will see below, very long relaxation times in zero field, no longer limited by field inhomogeneities. The residual stray static fields inside the shield (about 10^{-6} G) are compensated by sets of Helmholtz coils. The ^{3}He atoms are optically pumped by a circularly polarized light beam B_2 ($\lambda = 10\,830$ Å) to achieve the orientation of the $^1S_0$ ground state by the classical technique.[3] The nuclear spins are oriented along the direction of B_2, and as long as there is no applied field, they remain in this direction.

The ^{87}Rb magnetometer[4] makes use of a new type of detection of the zero-field level-crossing resonances appearing in the ground state of optically pumped atoms.[5] The 6-cm-diam ^{87}Rb cell (without buffer gas), with paraffin-coated wall, is the magnetic probe of the magnetometer; it is placed close to the ^{3}He cell and optically pumped by the circularly polarized light beam B_1 (D_1 component of the resonance line) perpendicular to B_2. A rf field $\vec{H}_1 \cos\omega t$ is applied in the direction of B_2 ($\omega/2\pi = 400$ Hz). The transmitted light of B_1, measured by a photomultiplier, is modulated at various harmonics $p\omega$ of ω. The modulation ($p = 1$) is proportional to the component par-

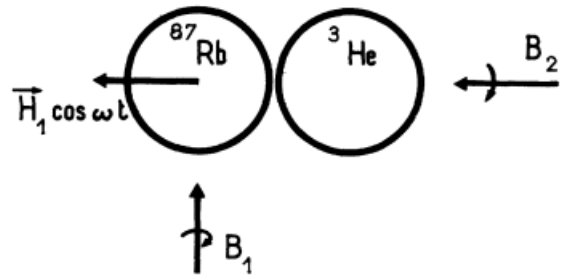

FIG. 1. Schematic diagram of the experimental arrangement.

cally. Finally, various applications of this method might be used to set up magnetometers or gyrometers.

External detection of ^{3}He

W. Heil “Helium Magnetometers”, Springer 2017
DOI:10.1007/978-3-319-34070-8_16

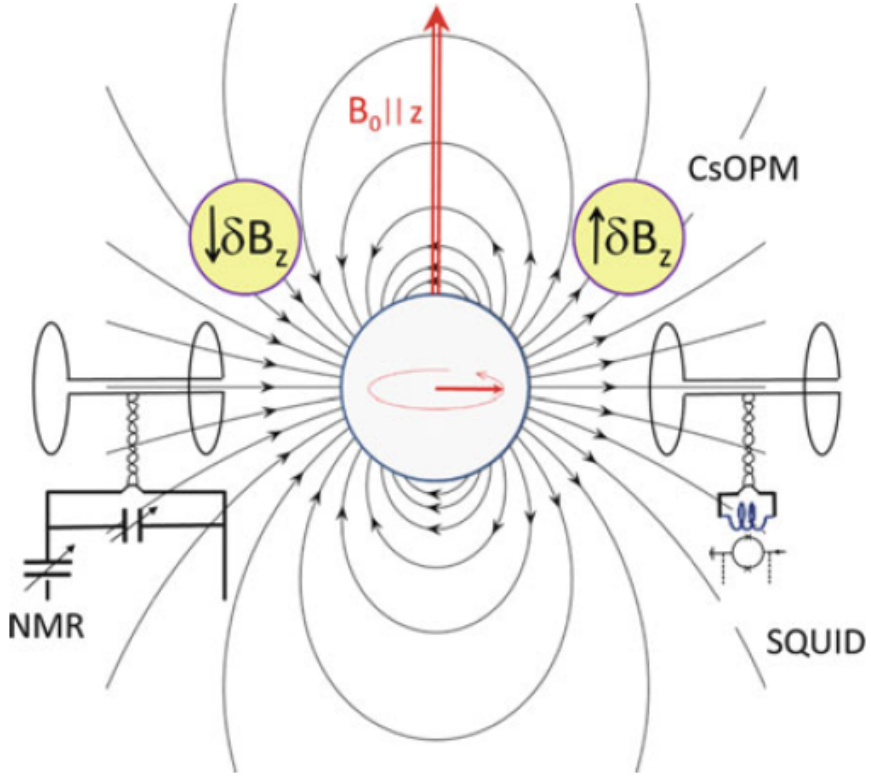

Fig. 7 Schematic layout of the He-3 nuclear magnetometer based on free spin precession. The ^{3}He magnetization in a spherical sample cell produces a dipolar field distribution outside the cell. As readout of the rotating magnetization three types of gradiometer systems are shown: **a** low-T_c SQUIDs, **b** Cs optical pumped magnetometers (CsOPM), and **c** NMR detection. Whereas (**a**) and (**b**) are used at $B_0 < 50$ μT, magnetic measurements via NMR are preferable at high magnetic fields ($B_0 > 0.1$ T). For details see text

MEOP ^{3}He detected by Alkali

H. C. Koch , “Design and performance of an absolute ^{3}He/Cs Magnetometer”, Euro. Phys. J. D 2015
DOI:10.1140/epjd/e2015-60018-7

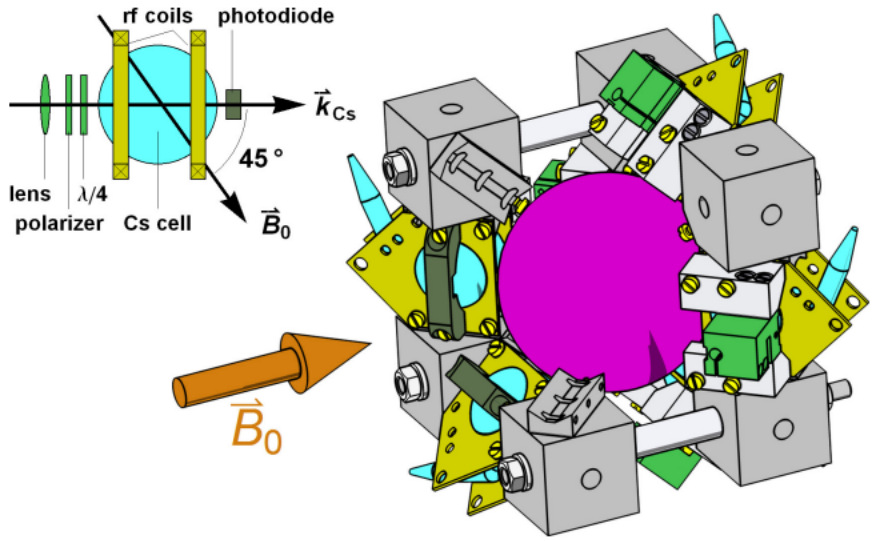

Fig. 2. (Color online) Schematic drawing of the CsOPM (left) and CAD drawing of the combined ^{3}He/Cs magnetometer (right). The spherical ^{3}He cell (magenta) in the middle of the cubic structure is surrounded by eight CsOPMs (blue) on the edges of the cube, in which the rf coils are laid out on printed circuit boards (yellow). The total dimensions of the combined magnetometer are $\sim (10\,\mathrm{cm})^3$. One corner cube and two CsOPMs are left out for better visibility.

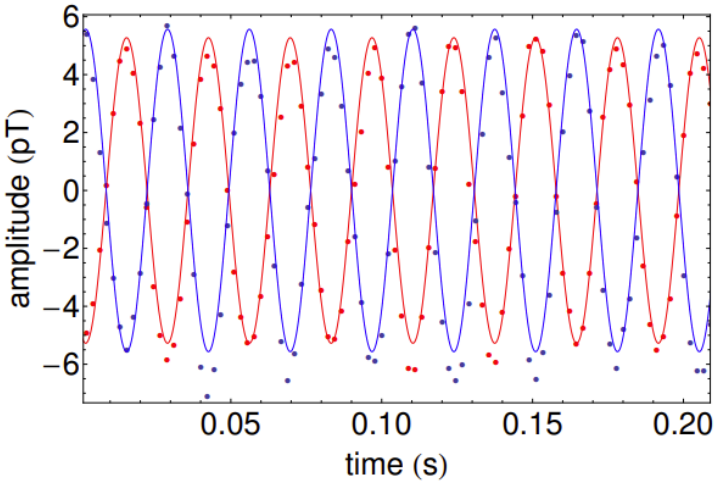

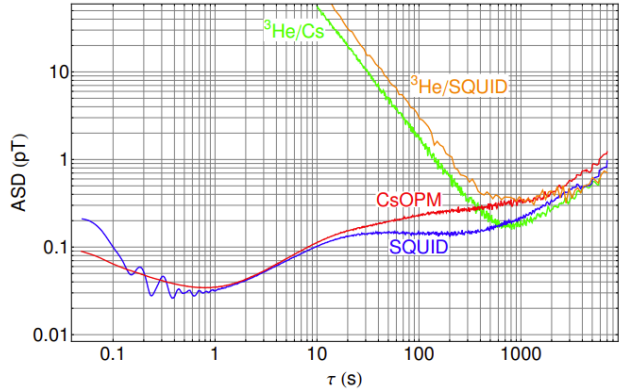

Fig. 10. (Color online) Allan standard deviation of simultaneous field measurements with the ^{3}He/Cs (green), the CsOPM (red), the SQUID (blue) magnetometer, and the ^{3}He/SQUID (orange) respectively. For long integration times the sensitivity of all magnetometers is limited by a common noise process.

MEOP/SEOP ^{3}He detected by Alkali

W/ T. Chupp, detection of polarized ^{3}He by scalar pulsed ^{87}Rb gradiometer at 2.5 μT,

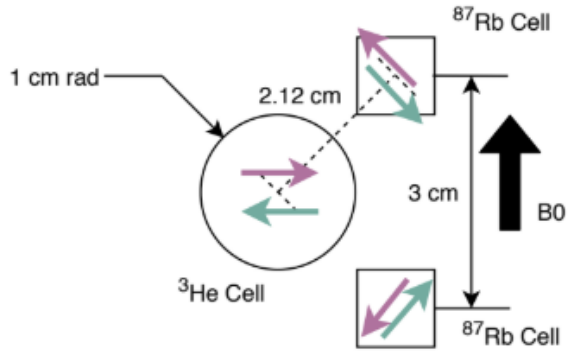

FIG. 1. Schematic of experimental apparatus with fields generated due to ^{3}He cell at each ^{87}Rb cell.

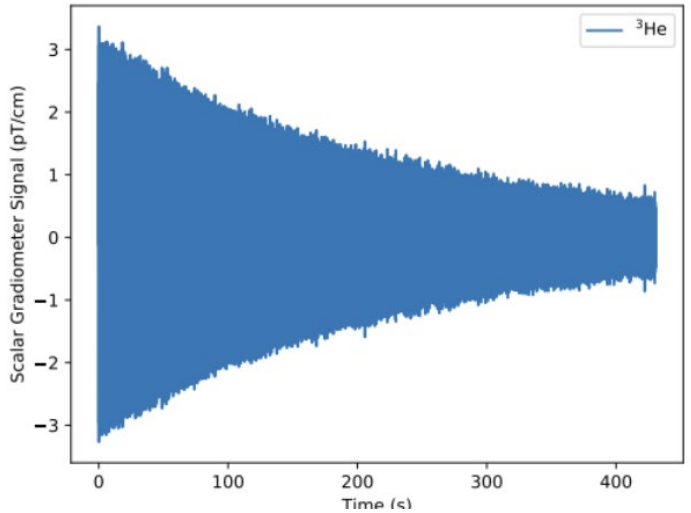

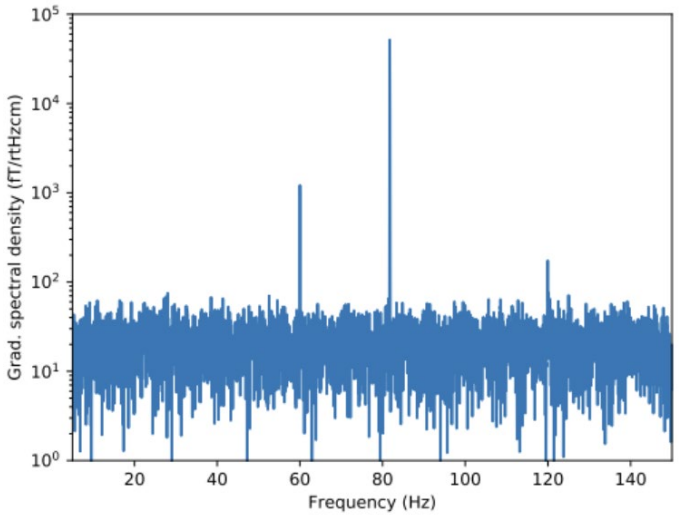

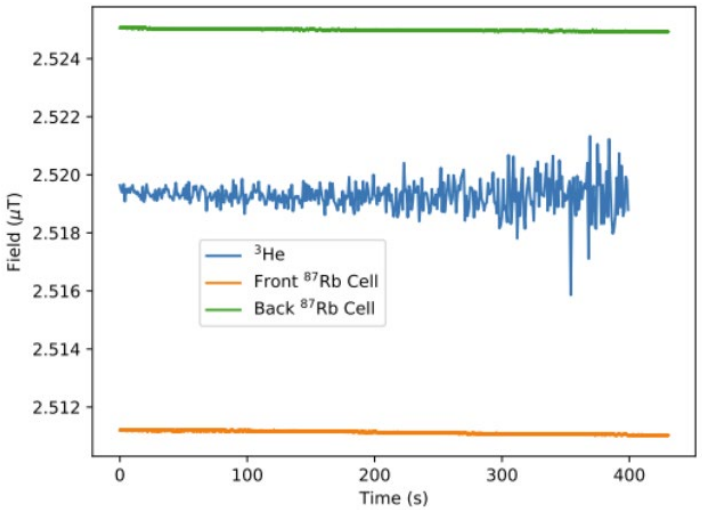

Mike Romalis

Limes, et al., "Portable Magnetometer for Detection of Biomagnetism in Ambient Environments", PRApplied, 2020, DOI: 10.1013/PhysRevApplied.14.011002

Magnetometry Tutorial

- General Magnetometry
- Optical Pumping of Metastable Noble gas electronic states (2^3S_1 in ^4He),

  direct optical read-out
- Metastability Exchange Optical Pumping (MEOP) of Noble gas Nuclei,
- Spin Exchange Optical Pumping (SEOP) of Noble gas Nuclei,

  both external read-out via:

  a) coils

  b) SQUIDs or

  c) atoms (can use atoms for in-situ measurements, optically detected)

Spin-Exchange Optical Pumping

Bouchiat, Carver, Varnum, "Nuclear polarization in ^{3}He Gas induced by optical pumping and dipolar exchange", PRL , (1960) DOI:10.1103/PhysRevLett.5.373

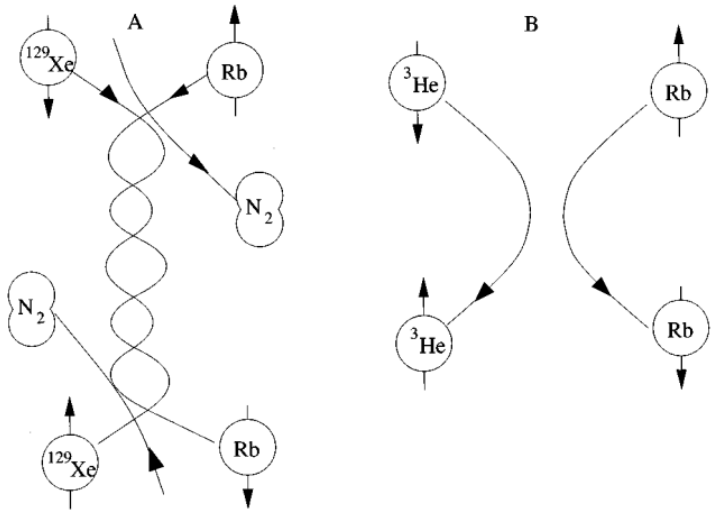

FIG. 8. Polarization transfer processes. (a) Formation and breakup of an alkali-metal/noble-gas van der Waals molecule. (b) Binary collision between an alkali-metal atom and a noble-gas atom.

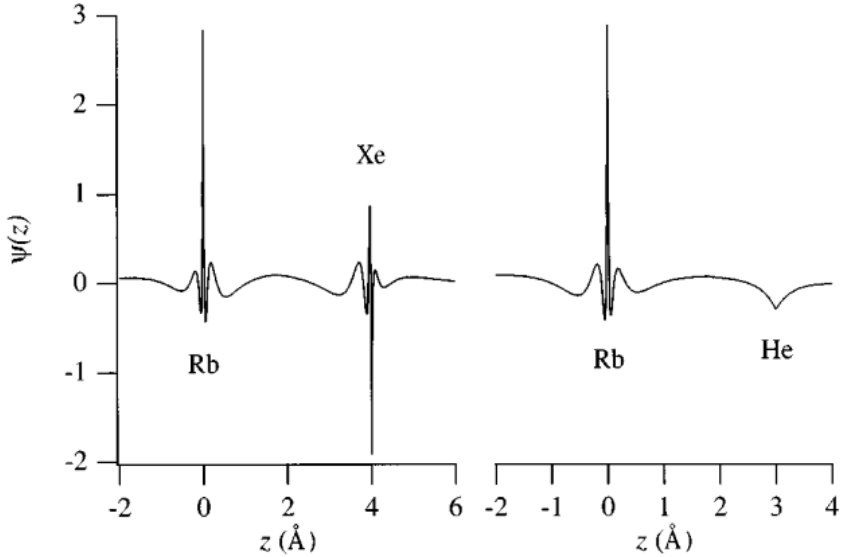

FIG. 13. The valence-electron wave function ψ of Rb-He and Rb-Xe as a function of position along the internuclear axis.

Walker, Happer, "Spin-exchange optical pumping o
noble-gas nuclei", RMP Colloqiua, (1997)
DOI:10.1103/RevModPhys.69.629

SEOP 3He can be 'slower' to pump up nuclei to steady state than MEOP, but SEOP can accommodate large pressures and the rest of the spin-ful noble gas nuclei

SEOP Coil Detection

Saam lab at Utah
c. 2010

Low field NMR ~2 mT
Of ^{129}Xe gas cells

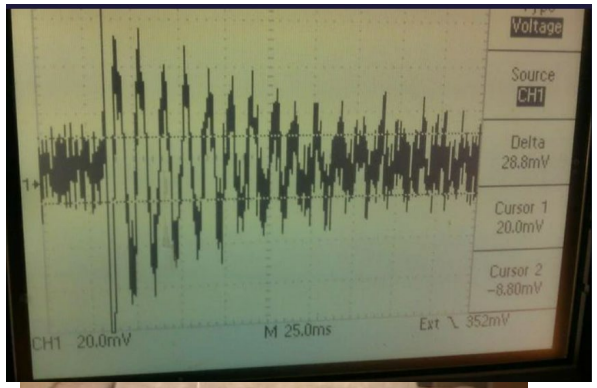

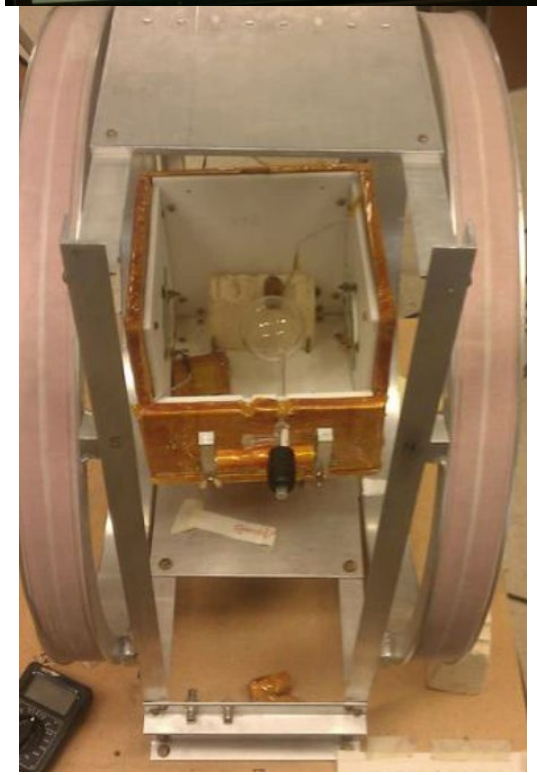

Flow-through Xe polarizer

Co-magnetometers

Noble gas nuclei well-isolated -> very long coherence times

Spin is an inertial system … can we make a gyro?

Spin-1/2 Hamiltonian $\gamma B \cdot S$ -> can't tell the difference between magnetic field drift and rotation of apparatus around spins

Solution: Use two spin species, and become insensitive to magnetic field drifts

From long integration time, can also achieve very low energy resolutions for tests of exotic spin-dependent interaction

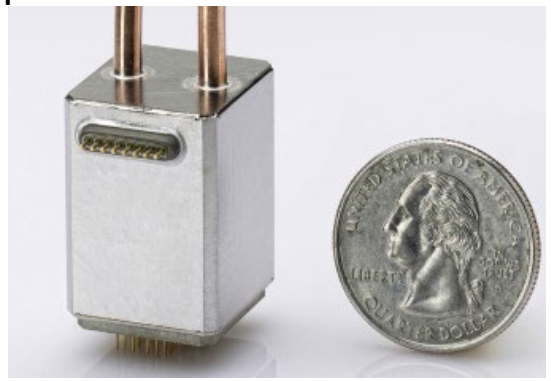

T. Walker, M. S. Larsen,
"Spin-Exchange-Pumped NMR Gyros ", 2016,
DOI:10.1016/bs.aamop.2016.04.002

NYT, WASHINGTON, Aug. 16 (1963) - A new gyroscope, for which patents will be issued next month, uses the spin of the atom. Under an Air Force contract, General Precision, Inc., has built an experimental model.

Gyroscopes are used as stabilizers in aircraft and space vehicles. The conventional type has a whirling disk or wheel that resists being pushed off its axis.
The nuclear gyroscope uses the characteristic of certain atoms in which the nucleus behaves like a spinning top. As far as the inventors know, this is the first practical application of the principle.
Because the instrument has no moving parts, requires no power and withstands heavy shocks and vibrations, it is expected to have an indefinite life and to be useful on spacecraft during deep probes and on long-range satellites.
The heart of the gyroscope is an absorption cell made of fused quartz and containing an invisible amount of mercury vapor. The "isotopically enriched" mercury would cost $40,000,000 a pound, according to the company. But such tiny quantities are used that the cost is only $20 a cell.

The G.P.L. division of General Precision, Inc., at Pleasantville, N. Y., began study of the nuclear gyroscope in 1957. The recent work has been conducted by a team headed by Dr. James H. Simpson, Jr., in cooperation with scientists of the Air Force Aeronautical Systems Division, Wright-Patterson Air Force Base, Ohio.
Four patents, obtained for General Precision by Dr. Simpson, Ivan A. Greenwood, Jr., John P. Lowdenslager and Julius T. Fraser, will be issued Sept. 10.


New Gyroscope Uses the Spin of Atoms

SEOP MASER/Detection

T.E. Chupp, R. Walsworth et al., "Spin-exchange-pumped ^{3}He and ^{129}Xe Zeeman Masers", PRL, 1994, DOI:10.1103/PhysRevLett.112.110801

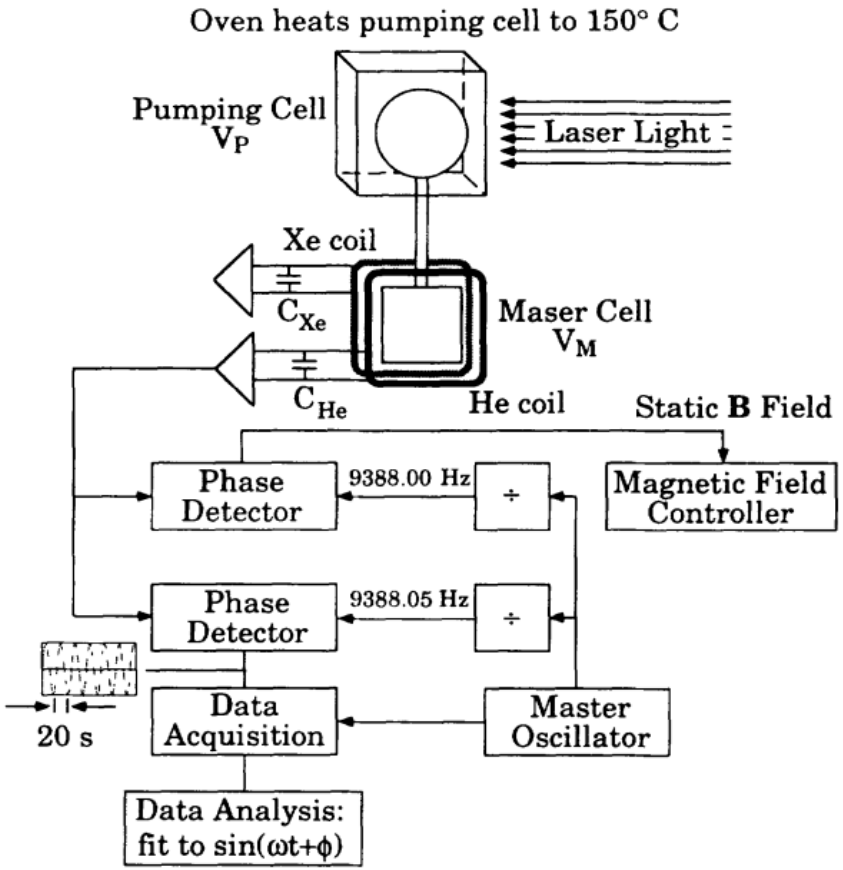

D. Bear, et al., "Improved frequency stability of the dual-noble-gas maser", PRA, 1998, DOI:10.1103/PhysRevA.57.5006

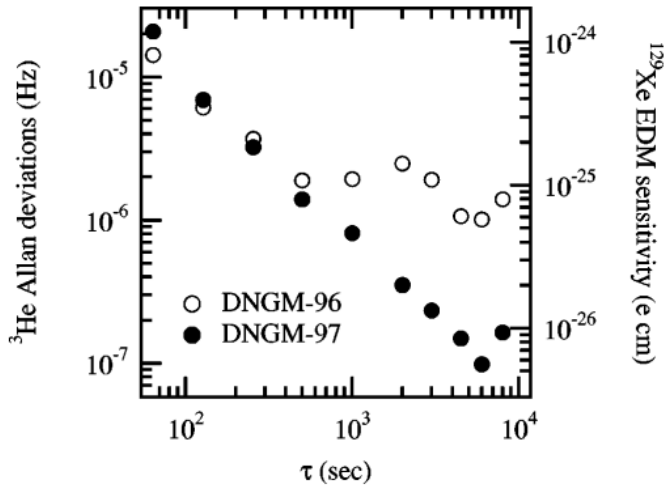

FIG. 2. Comparison of measured frequency stabilities (Allan deviations) for the free-running ^{3}He masers in the current and previously reported dual noble-gas masers. The Allan deviation of the earlier system reached a rough ''floor'' at ~1–2 μHz for measurement intervals of approximately thousands of seconds. The Allan deviation of the current dual noble-gas maser is substantially smaller, decreasing to ~100 nHz for measurement intervals of ~6000 s. Sensitivity to changes in the ^{129}Xe Zeeman frequency is given by dividing the free-running ^{3}He maser frequency stability by ~2.7, the ratio of ^{3}He and ^{129}Xe magnetic moments. The right ordinate axis shows the one standard deviation sensitivity to a ^{129}Xe permanent electric dipole moment, as a function of measurement interval τ, that would result from (i) a free-running ^{3}He maser frequency measurement with the Allan deviation given on the left ordinate axis; and (ii) the alternate application of electric fields of +5 kV/cm and –5 kV/cm across the maser bulb, alternating the field direction every τ seconds. (This is a simplistic sensitivity estimate, and ignores potential difficulties associated with electric fields, etc.)

SEOP ^{3}He + ^{129}Xe detected by SQUIDs

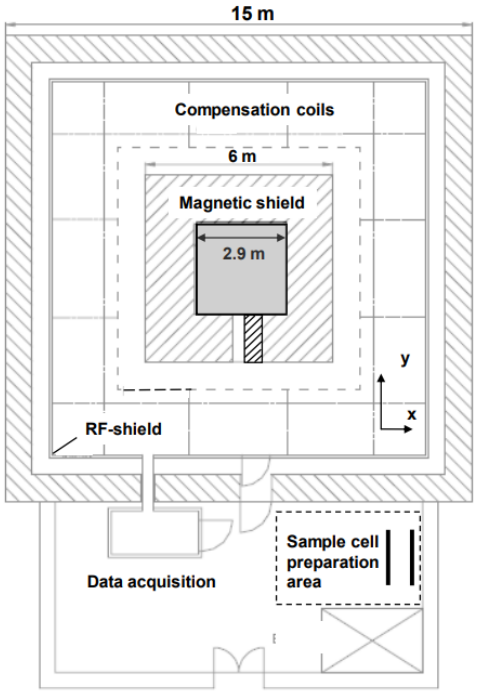

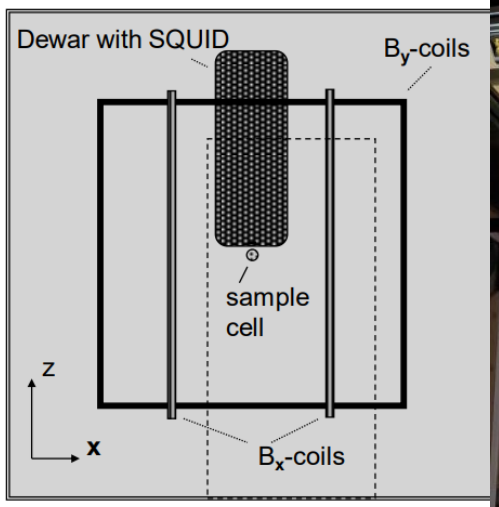

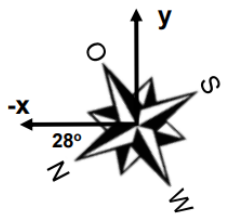

C. Gemmel, et al., "Ultra-sensitive magnetometry based on free precession of nuclear spins", Euro. Phys. J. D, 2010, DOI:10.1140/epjd/e2010-00044-5

F. Allmendinger, et al., "New limit on Lorentz and CPT violating neutron spin interactions using a free precession ^{3}He-^{129}Xe co-magnetometer", PRL, 2013, DOI:10.1103/PhysRevLett.112.110801

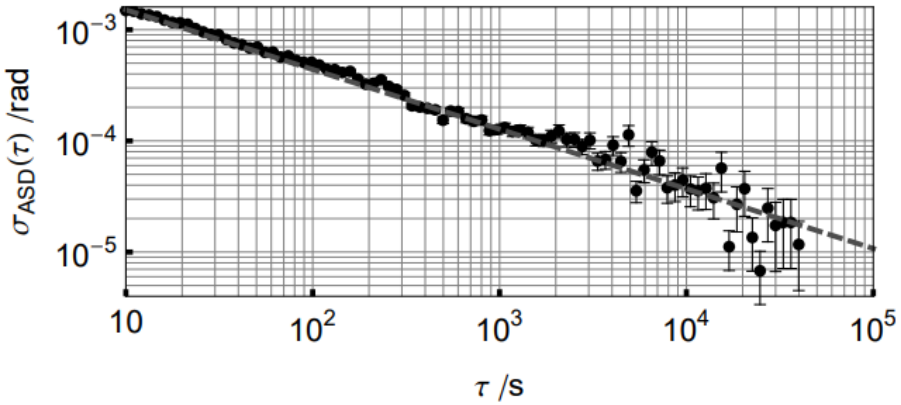

FIG. 2. Allan Standard Deviations (ASD) of the residual phase noise of a single run ($j = 6$). The total observation time was $T = 90000$ s. With increasing integration times τ the uncertainty in phase decreases as $\propto \tau^{-\frac{1}{2}}$ indicating the presence of white phase noise.

SEOP noble gases detected by in situ Alkali

B. C. Grover, "Noble-Gas NMR Detection through Noble-gas-rudium Hyperfine contact interaction", PRL (1978) DOI:10.1016/0029-554X(73)90698-8

The use of optically pumped Rb vapor to transfer polarization to a second atomic species through spin-exchange collisions is well known[1] and was first used to polarize a noble gas (NG) by Bouchiat, Carver, and Varnum[2] in their work with ^{3}He. The method has been extended in this laboratory to include all the stable NG isotopes.

Several methods have been used for the detection of NG nuclear magnetism polarized through spin exchange with Rb: measurement of the induced voltage in rf detection coils in a NMR experiment in the case[2,3] of ^{3}He and also in the case[4] of ^{129}Xe, and direct observation of the magnetic dipole field of the oriented nuclei by an adjacent ^{87}Rb magnetometer.[5] For my detection scheme, I also use a Rb magnetometer mechanized in the zero-field level-crossing mode[6]; however, here the Rb atoms within the mixed Rb-NG sample cell comprise the magnetometer sensor. By this method I have successfully observed enhancement of the nuclear polarization in the NG isotopes ^{3}He, ^{21}Ne, ^{83}Kr, ^{129}Xe, and ^{131}Xe.

The experimental setup consists of a 15-ml Pyrex sphere filled with Rb metal, a buffer gas of ^{4}He at 500 Torr, and one or more species of NG at a pressure on the order of 1 Torr. The cell is contained within a resistance-heated oven provided with Pyrex windows at either end. The oven is capable of controlled temperatures to 85°C. A three-axis set of Helmholtz coils surrounds the oven, and the whole assembly is placed within a cylindrical magnetic shield which reduces external magnetic fields to below 10 μG. The Rb atoms

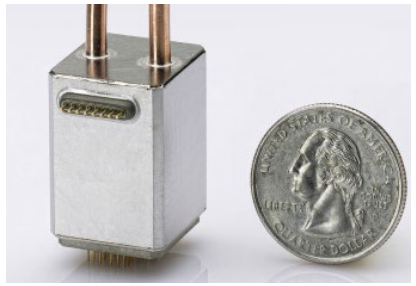

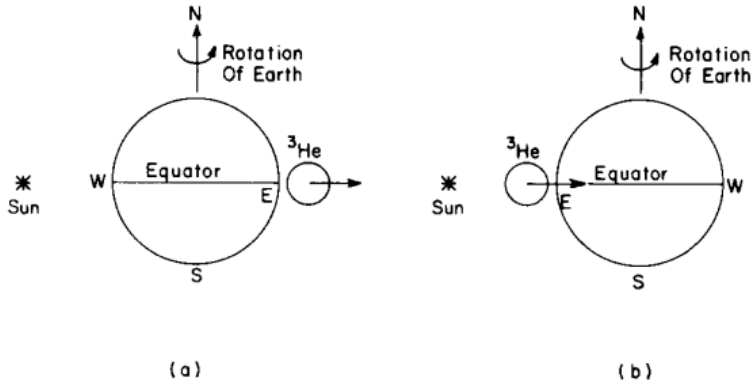

Fig. 16. An alternative to the Foucault pendulum.

A. Kastler, "The Hanle Effect and its Use for the Measurements of Very Small Magnetic Fields", Nuclear Inst. And Methods (1973) DOI:10.1016/0029-554X(73)90698-8

J. Brown , "A New Limit on Lorentz- and CPT-Violating Neutron Spin Interactions Using a K-3He Comagnetometer", Dissertation, 2011

Self-compensating comagnetometer

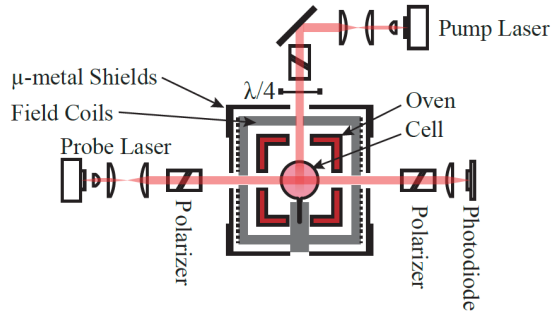

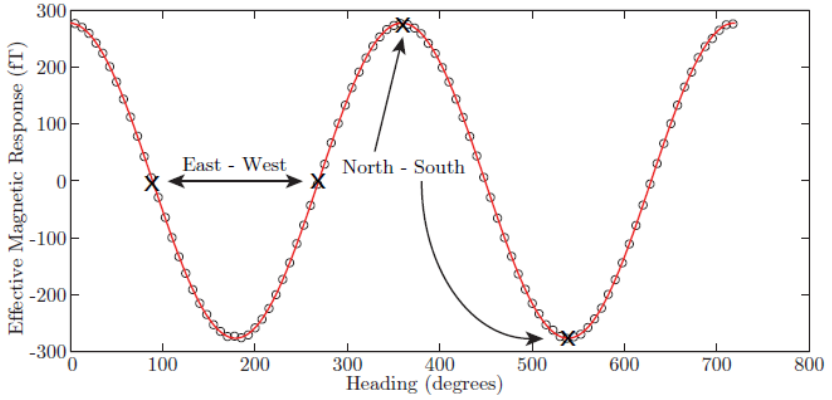

Figure 3.16: Earth's rotation as a function of heading of the comagnetometer. Each point represents 8 reversals of the apparatus. Error bars are smaller than the size of each point and are omitted. The curve is a fit with an amplitude of 277 fT and phase of 1.1°W of the expected direction. Rotation conventions are discussed in Section 4.1.1.

SEOP noble gases detected by in situ Alkali

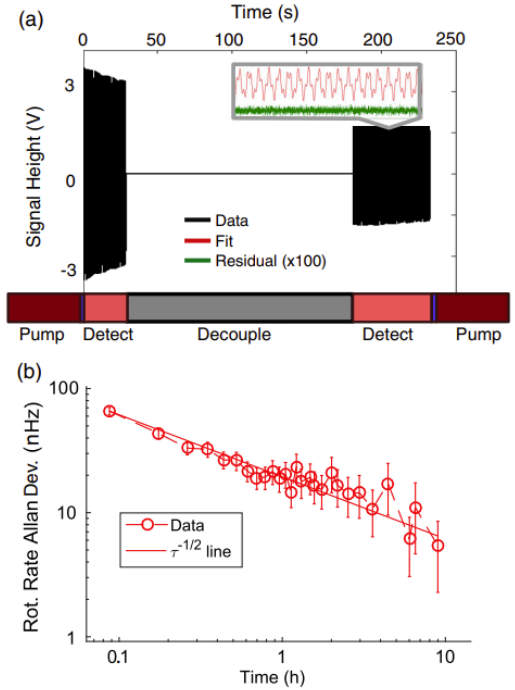

FIG. 3. (a) The Ramsey scheme with an inset showing a ^{3}He-^{129}Xe lock-in signal pattern and the fit residuals ×100. (b) Allan deviation of the rotation rate Ω_z with an 7 nHz (10^{-2} deg /h) upper limit of the rotation rate stability.

Free-precession, dual spin-1/2 comagnetometer

M. E. Limes, D. Sheng, M. V. Romalis "^{3}He-^{129}Xe Comagnetometry using ^{87}Rb Detection and Decoupling", PRL (2018) DOI:10.1103/PhysRevLett.120.033401

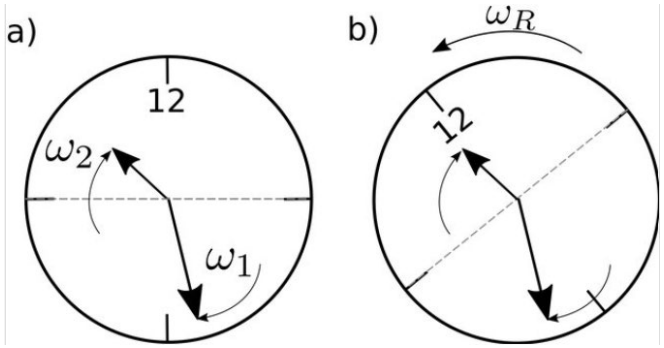

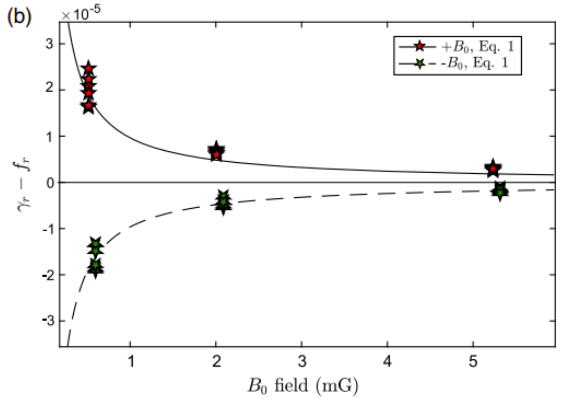

Frequency ratio plotted for field with and against projection on Earth's rotation axis, along with parameter free model

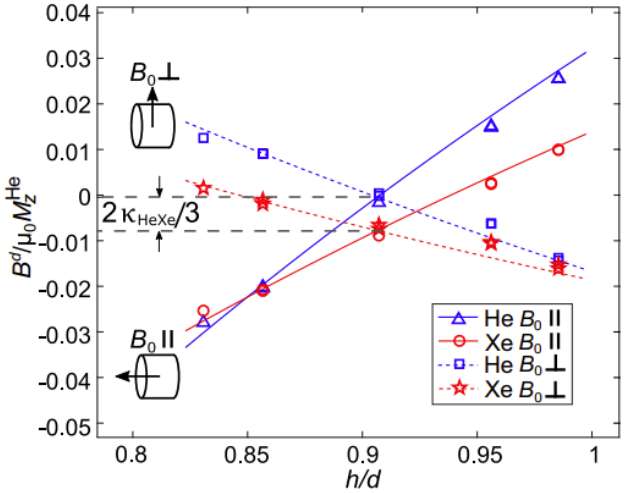

FIG. 3. The slope $B^d/\mu_0 M_z^{He}$ is plotted against the cell aspect ratio h/d for B_0 ∥ and B_0 ⊥ to the cylinder axis. Lines show dipolar field theory with only κ_{HeXe} as a free parameter.

Detected J coupling between ^{3}He and ^{129}Xe!

$$J\boldsymbol{I}_{He} \cdot \boldsymbol{I}_{Xe}$$

M. E. Limes, M. V. Romalis, et al. "Dipolar and scalar ^{3}He-^{129}Xe frequency shifts in stemless cells", PRA (2019) DOI:10.1103/PhysRevA.100.010501

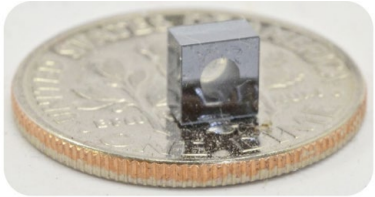

SEOP noble gases detected by in situ Alkali

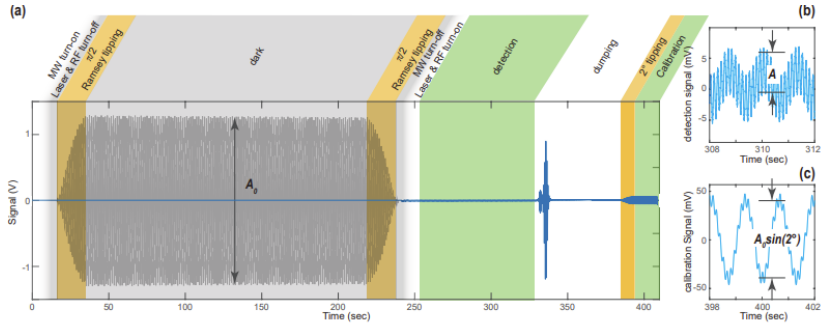

FIG. 1. (a) Schematic of the in-the-dark operation of the nuclear spin comagnetometer. The gray solid lines illustrate the evolution of the two nuclear spins under the Ramsey scheme, while blue lines indicate recorded signals. The detection time is approximately equal to half of the free precession time to yield the optimal Cramér–Rao lower bound. (b) and (c) Nuclear spin precession signals during the detection stage and after a 2° calibration pulse. The amplitudes A_0 and A are obtained separately for each nuclear spin, with only the ^{21}Ne amplitude indicated in the figure.

Free-precession, closer to an actual Ramsey scheme
ARW <0.002 deg/h$^{1/2}$, bias drift < 0.001 deg/h!

S. Zhang, M. V. Romalis, et al., "A ^{3}He-^{21}Ne Ramsey Comagnetometer with sub-nHz frequency resolution (2025) DOI:arXiv:2509.13486, 2025

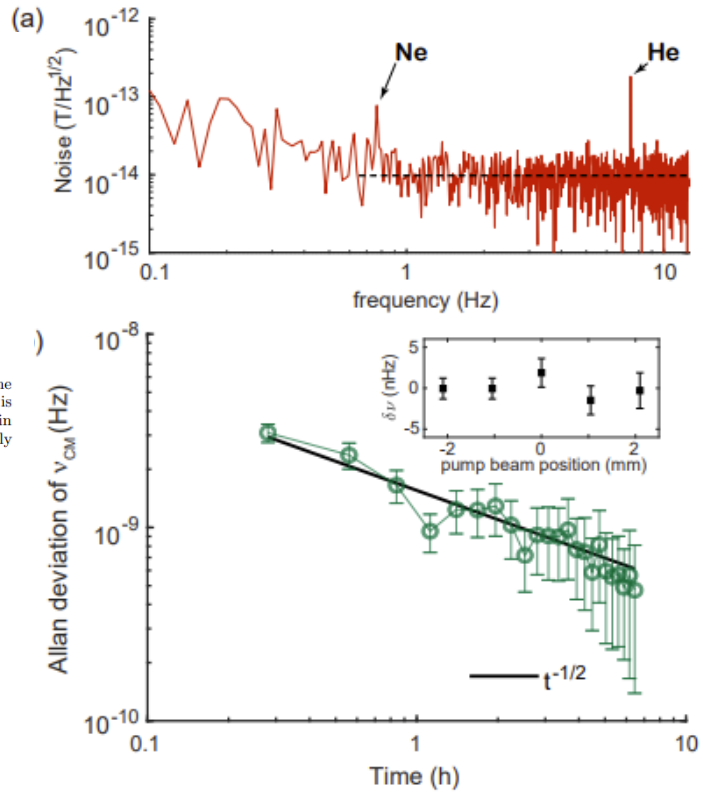

FIG. 4. (a) Frequency spectrum of the pulse train Rb magnetometer, showing examples of small residual signals from Ne and He spin precession. (b) Allan deviation of the comagnetometer frequency, showing an upper stability limit of 580 pHz. The sensitivity to inertial rotation is equal to $0.002°/\sqrt{\text{h}}$. Inset: Stability of the comagnetometer under deliberate pump laser misalignment from the cell center.

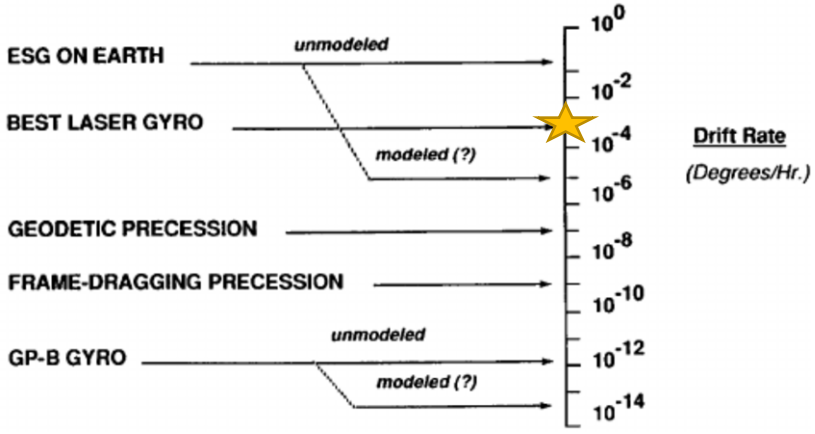

Detection of noble gases for magnetometry

External: Raw sensitivity can be limited by distance to center (A uniformly magnetized sphere behaves like a pure magnetic dipole at its center, $B \propto \frac{1}{r^3}$)
Although, sensitivity is often not the limiting factor for long-term bias drift

In-situ alkali: Provides enhanced signals through Fermi-contact interaction, can be nuclear spin-noise limited, but need to tame/exploit field shifts introduced by polarized or (back-polarized) alkali

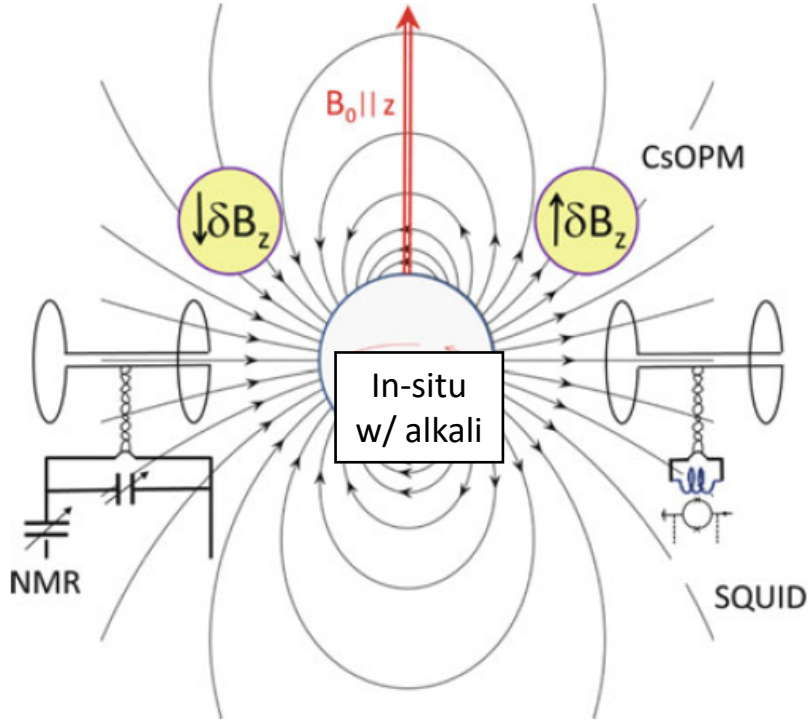

Fig. 7 Schematic layout of the He-3 nuclear magnetometer based on free spin precession. The ^{3}He magnetization in a spherical sample cell produces a dipolar field distribution outside the cell. As readout of the rotating magnetization three types of gradiometer systems are shown: **a** low-T_c SQUIDs, **b** Cs optical pumped magnetometers (CsOPM), and **c** NMR detection. Whereas (**a**) and (**b**) are used at $B_0 < 50$ μT, magnetic measurements via NMR are preferable at high magnetic fields ($B_0 > 0.1$ T). For details see text

W. Heil "Helium Magnetometers", Springer 2017
DOI:10.1007/978-3-319-34070-8_16

Polarization in Noble Gases 2026
Magnetometry Tutorial

Limes Atomic Physics Lab Aug. 2024

Mark Limes
Associate Prof.
Virginia Tech
4/22/2026


Limes Atomic Physics Lab Sept. 2025